SLAC-PUB-17058

CERN-PH-EP-2011-079
submitted to journal

Prepared for submission to JHEP

Measurement of $W\gamma$ and $Z\gamma$ production in proton-proton collisions at $\sqrt{s} = 7$ TeV with the ATLAS Detector

The ATLAS Collaboration [1]

Abstract: We present studies of W and Z bosons with associated high energy photons produced in pp collisions at $\sqrt{s} = 7$ TeV. The analysis uses 35 pb^{-1} of data collected by the ATLAS experiment in 2010. The event selection requires W and Z bosons decaying into high p_{T} leptons (electrons or muons) and a photon with $E_{\mathrm{T}} > 15$ GeV separated from the lepton(s) by a distance $\Delta R(l, \gamma) > 0.7$ in η-ϕ space. A total of 95 (97) $pp \to e^{\pm}\nu\gamma + X$ ($pp \to \mu^{\pm}\nu\gamma + X$) and 25 (23) $pp \to e^{+}e^{-}\gamma + X$ ($pp \to \mu^{+}\mu^{-}\gamma + X$) event candidates are selected. The kinematic distributions of the leptons and photons and the production cross sections are measured. The data are found to agree with Standard Model predictions that include next-to-leading-order $O(\alpha\alpha_s)$ contributions.

Keywords: Hadron-Hadron Scattering

[1] See Appendix for the list of collaboration members

This material is based upon work supported by the U.S. Department of Energy, Office of Science, under Contract No. DE-AC02-76SF00515.

Contents

1 Introduction

Measurements of the production of W and Z bosons with associated high energy photons provide important tests of the Standard Model (SM) of particle physics. The $W\gamma$ process is directly sensitive to the triple gauge boson couplings predicted by the non-Abelian $SU(2)_L \times U(1)_Y$ gauge group of the electroweak sector. The triple gauge boson couplings in the $Z\gamma$ process vanish in the SM at tree level. Physics beyond the SM such as composite structure of W and Z bosons, new vector bosons, and techni-mesons would enhance production cross sections and alter the event kinematics. Data taken with the ATLAS detector [1] provide a new opportunity to study $W\gamma$ and $Z\gamma$ production using the high energy pp collisions provided by the Large Hadron Collider (LHC). Previous hadroproduction measurements have been made at the Fermilab Tevatron collider by the CDF [2] and D0 [3] collaborations using $p\bar{p}$ collisions at $\sqrt{s} = 1.96$ TeV and at LHC by the CMS [4] collaboration.

Our studies use measurements of $pp \to l^{\pm}\nu\gamma + X$ and $pp \to l^{+}l^{-}\gamma + X$ production at $\sqrt{s} = 7$ TeV with an integrated luminosity of approximately 35 pb^{-1}. Events are selected by requiring the presence of a W or Z boson candidate along with an associated isolated photon having a transverse energy $E_{\mathrm{T}} > 15$ GeV and separated from the closest electron or muon l by $\Delta R(l, \gamma) > 0.7$ [1].

The sources of the $l^{\pm}\nu\gamma$ and $l^{+}l^{-}\gamma$ final states are $W\gamma \to l^{\pm}\nu\gamma$ and $Z\gamma \to l^{+}l^{-}\gamma$ production, as well as QED final state radiation from inclusive W and Z production: $W \to l^{\pm}\nu \to l^{\pm}\nu\gamma$, $Z \to l^{+}l^{-} \to l^{+}l^{-}\gamma$ (Fig. 1). The data also include events with photons coming from hard fragmentation of a quark or gluon (see Fig. 2 for the case of $l\nu\gamma$). This source, while reduced by the photon identification and isolation requirements, cannot be neglected and is considered as a part of the signal process in the analysis presented here. Throughout this document the label "Z" refers to Z/γ^* [2] and the notations $W\gamma$ and $Z\gamma$ are used to denote the $l^{\pm}\nu\gamma$ and $l^{+}l^{-}\gamma$ final states.

2 Monte Carlo Simulations of Standard Model Predictions for the $W\gamma$ and $Z\gamma$ Signal and Backgrounds

Monte Carlo (MC) event samples with full ATLAS detector simulation are used for comparisons of the data to the theoretical expectations for the $W\gamma$ and $Z\gamma$ signals and various backgrounds. In this section the details of the MC event generators are described.

Since next-to-leading-order (NLO) generators with parton shower simulation are not available for the $W\gamma$ and $Z\gamma$ signal processes, they are generated with a MADGRAPH [5] leading-order (LO) matrix-element generator interfaced to PYTHIA [6] for gluon radiation

[1] The nominal interaction point is defined as the origin of the coordinate system, while the anti-clockwise beam direction defines the z-axis and the $x - y$ plane is transverse to the beam direction. The positive x-axis is defined as pointing from the interaction point to the centre of the LHC ring and the positive y-axis is defined as pointing upwards. The azimuthal angle ϕ is measured around the beam axis and the polar angle θ is the angle from the beam axis. The pseudorapidity is defined as $\eta = -\ln tan(\theta/2)$. The distance ΔR in the $\eta - \phi$ space is defined as $\Delta R = \sqrt{\Delta\eta^2 + \Delta\phi^2}$

[2] γ^* denotes an off-shell photon.

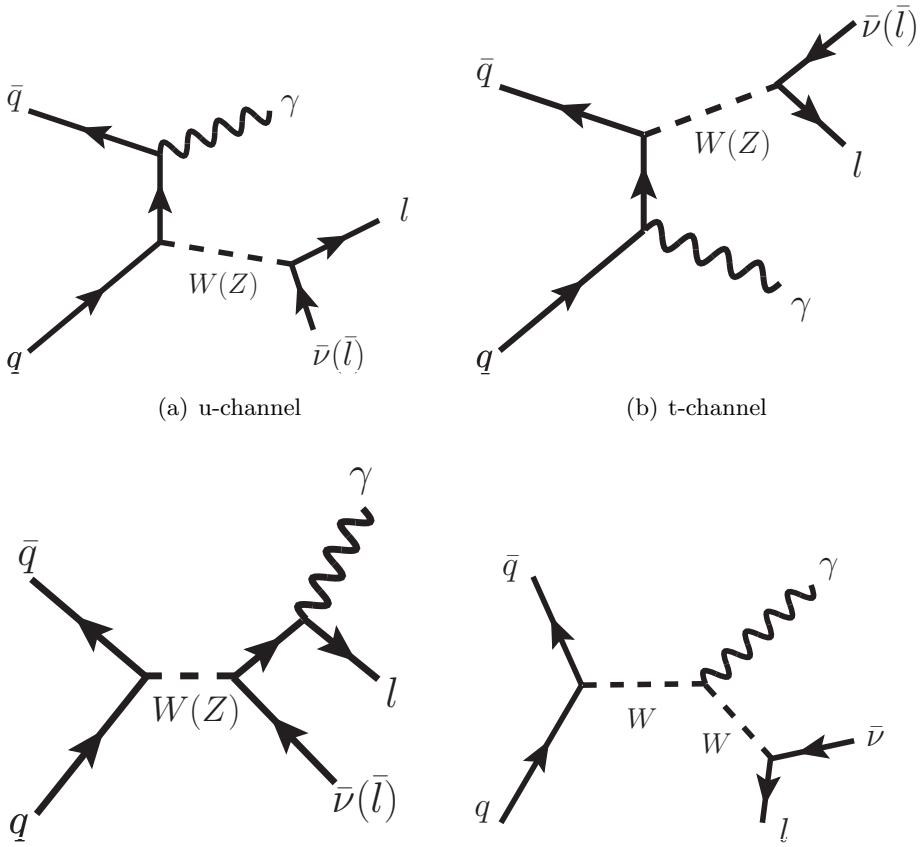

Figure 1. Feynman diagrams of $W\gamma$ and $Z\gamma$ production in (a) u-channel (b) t-channel and (c) final state photon radiation (FSR) from the W and Z boson decay process. (d) Feynman diagram of $W\gamma$ production in the s-channel.

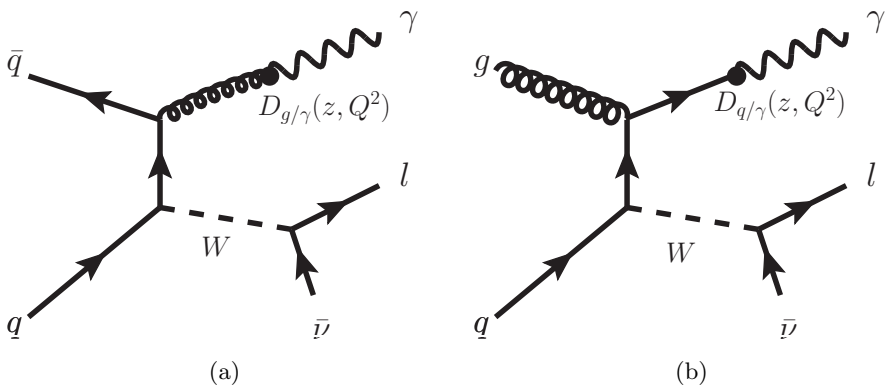

Figure 2. Diagrams of the signal contributions from the $W+q(g)$ processes when a photon emerges from the fragmentation of the final state parton.

and hadronization, and PHOTOS [7] for photon radiation off the electron or muon in the W and Z decay. The simulations of the signal processes using the MADGRAPH generator

include interference effects between amplitudes, and effects from boson decay widths. The matrix-element calculation uses the leading-order parton distribution function (PDF) sets CTEQ6L1 [8], and the corresponding ATLAS MC tune 2009 [9]. Both the $W\gamma$ and $Z\gamma$ MADGRAPH samples are generated with photon $E_{\mathrm{T}} > 10$ GeV and $\Delta R(l,\gamma) > 0.5$.

Fig. 1 illustrates the dominant sources of $W\gamma$ and $Z\gamma$ events. The final state radiation (FSR) from $W\gamma$ ($Z\gamma$) events are identified with a cut on the invariant mass of the lepton-neutrino (opposite charged di-lepton) at the parton generator level. Those $W\gamma$ ($Z\gamma$) events with $m(l\nu) < 74$ GeV ($m(ll) < 85$ GeV) are categorized as FSR. The remaining events are identified as initial state radiation events (ISR). The $W\gamma$ and $Z\gamma$ ISR events include those with photon radiation from initial state quarks, and for $W\gamma$ production, from the $WW\gamma$ vertex(see Fig. 1 (d)). The division of the generated LO events into FSR and ISR categories is needed in order to apply the higher order perturbative corrections described below.

There are significant modifications to the LO electroweak $W\gamma$ and $Z\gamma$ cross sections due to QCD corrections, as in the case of inclusive W and Z boson production. To introduce QCD corrections, our approach is to weight the fully simulated LO MC events with NLO k-factors. NLO predictions considering both QED and QCD vertices ($O(\alpha\alpha_S)$) are determined using the Baur program [10, 11], a matrix element parton generator with complete next-to-leading-logarithm diagrams for $W\gamma$ and $Z\gamma$ production using narrow width approximations for the W and Z bosons. The NLO Baur calculations for $W\gamma$ and $Z\gamma$ di-boson production do not include FSR off the decay leptons. Therefore a k-factor k_{ISR} determined by comparing the Born level and the NLO Baur MC calculations, is applied to LO events identified as ISR as described above. For the FSR LO event weighting a k_{FSR} is determined using an inclusive W/Z NLO calculation with the assumption that inclusively produced bosons have the same production dynamics as those with radiation off the decay leptons. To suppress photon signal contributions from quark/gluon fragmentation [12] (see Fig. 2 for the case of $l^{\pm}\nu\gamma$) isolation cuts are applied to the photons selected in the $W\gamma$ and $Z\gamma$ data and those from simulated quark/gluon fragmentation in the NLO generator. The events used for the NLO k-factor calculation and for the theoretical cross section predictions are generated with $\epsilon_h < 0.5$, where ϵ_h is an isolation criterion at generation level. The variable ϵ_h (ϵ_h^p) is used for the definition of isolated photons, at the parton (particle) level and is defined as the ratio of the sum of energies carried by the partons (particles) emerging from the quark/gluon fragmentation processes (excluding the photon) to the energy carried by the fragmented photon. The isolation criteria are applied using an $\eta - \phi$ cone of 0.4 centered on the photon. With these isolation cuts the quark/gluon fragmentation photons are estimated to contribute about 8% of the photons in the generated $W\gamma$ and $Z\gamma$ events.

In comparing the data to SM signal predictions, the background processes considered are W/Z+jets, $W \to \tau\nu$, $Z \to ll$ (background for the $W\gamma$), and $t\bar{t}$. The backgrounds from the production of single-top, direct single photon, dibosons ($WW/WZ/ZZ$) and QCD multi-jets are found to be negligible. We use the POWHEG [13] generator to simulate the $t\bar{t}$ production, with PYTHIA used to model parton showers. All other background sources are simulated with PYTHIA. For comparison to data, the cross sections for the background processes are normalized to the results of higher order QCD calculations. All signal and

background samples were generated at $\sqrt{s} = 7$ TeV, and then processed with a GEANT4 simulation of the detector [14]. The MC samples are simulated with on average two primary interactions but matched to data-taking conditions by weighting each event to obtain the primary vertex multiplicity distribution observed in data.

3 The ATLAS Detector

The ATLAS detector [1] consists of an inner tracking system (inner detector, or ID) surrounded by a thin superconducting solenoid providing a 2 T axial magnetic field, electromagnetic (EM) and hadronic calorimeters and by a muon spectrometer (MS). The ID is composed of three subsystems. The pixel (closest to the beam axis and with the highest granularity) and the silicon microstrip (SCT) detectors cover the pseudorapidity range $|\eta| < 2.5$, while the Transition Radiation Tracker (TRT) has an acceptance range of $|\eta| < 2.0$. The TRT provides identification information for electrons (and as a consequence also for photons that convert to electron-positron pairs) by the detection of transition radiation. The electromagnetic calorimeter is a lead liquid-argon (LAr) detector that is divided into one barrel ($|\eta| < 1.475$) and two end-cap components ($1.375 < |\eta| < 3.2$). The calorimeter consists of three longitudinal layers with the first (strip) having the highest granularity in the η direction, and the second collecting most of the electromagnetic shower energy. A thin presampler layer covering the range $|\eta| < 1.8$ is used to correct for the energy lost by EM particles upstream of the calorimeter. The transition region between the calorimeter and end-cap ($1.37 < |\eta| < 1.52$) is omitted for the detection of electrons and photons in this analysis. The hadronic calorimeter system, which surrounds the electromagnetic calorimeter, is based on two different detector technologies, with scintillator tiles or LAr as the active media, and with either steel, copper, or tungsten as the absorber material. The MS is based on three large superconducting aircore toroid magnets, a system of three stations of chambers for precise tracking measurements in the range $|\eta| < 2.7$, and a muon trigger system which extends to the range $|\eta| < 2.4$.

The ATLAS detector has a three-level trigger system. The first level trigger is largely based on custom built electronics that examine a subset of the total detector information to decide whether or not to record each event, reducing the data rate to below the design value of approximately 75 kHz. The subsequent two trigger levels run on a processor farm and look at more detector information with greater precision. They provide the reduction to a final data-taking rate designed to be approximately 200 Hz.

4 Data Samples

Events in this analysis were selected by triggers requiring at least one identified electron or muon candidate. The electron and muon trigger configurations changed during the data taking period in order to keep up with the increasing instantaneous luminosity delivered by the LHC. The strictest trigger selection criteria were applied in the last data taking period where leptons reconstructed at the third level of the trigger system were required to have $E_{\mathrm{T}} > 15$ GeV (electrons) and $p_{\mathrm{T}} > 13$ GeV (muons). Application of beam, detector,

and data-quality requirements resulted in a total integrated luminosity of 35.1 pb^{-1} (33.9 pb^{-1}) for the events collected with the electron (muon) trigger. The uncertainty on the absolute luminosity determination is 3.4 % [15, 16].

5 Reconstruction and Selection of $W\gamma$ and $Z\gamma$ Candidates

In this analysis the $W\gamma$ final state consists of an isolated electron or muon, large missing transverse energy due to the undetected neutrino, and an isolated photon. The $Z\gamma$ final state contains one pair of e^+e^- or $\mu^+\mu^-$ leptons and an isolated photon. Collision events are selected by requiring at least one reconstructed primary vertex consistent with the average beam spot position and with at least three associated tracks. The efficiency to reconstruct the primary vertex for $W\gamma$ and $Z\gamma$ events is 100%. The selection criteria for electrons, muons and transverse energy follow closely those used for the W and Z boson inclusive cross section analysis [17]. The selection criteria for the photon are similar to those used for the analysis of inclusive photon production [18].

5.1 Reconstruction of Electrons, Muons, Photons and Missing Transverse Energy

The muon candidates are reconstructed by associating the muon tracks in the MS to the tracks in the ID [17]. The combined track parameters of the muon candidates are derived using a statistical approach based on their respective errors. The selected muon candidate is a combined track from the primary vertex with $p_{\text{T}} > 20$ GeV and $|\eta| < 2.4$, and is isolated by requiring that the summed p_{T} of the tracks in a 0.4 radian cone around the muon candidate is less than 20% of the muon p_{T}. The p_{T} measured by the MS alone must be greater than 10 GeV. A quality cut based on the difference in the p_{T} measured independently in the ID and MS is applied to improve the purity of the muon candidates. To ensure a high quality track of the combined muon candidate, a minimum number of hits in the ID is required [19]. For the $W\gamma$ measurement in the muon channel, at least one muon candidate is required in the event, whereas for the $Z\gamma$ measurement, the selected events must have exactly two oppositely charged muon candidates.

The electron candidates are reconstructed from an electromagnetic calorimeter cluster associated with a reconstructed charged particle in the ID. The electron identification algorithm, which only considers electron candidates in the range $|\eta| < 2.47$ and excluding the region $1.37 < |\eta| < 1.52$, combines calorimeter and tracking information and provides three reference sets of selections ("loose", "medium" and "tight") with progressively stricter identification criteria and stronger jet rejection [17]. For the "medium" selection, information about the shower shape and width of the cluster, the quality of the associated track, and the cluster/track matching, as well as the energy deposited in the hadronic calorimeter are used for the identification. The "tight" selection uses in addition the ratio of cluster energy to track momentum, the particle identification potential of the TRT and stricter track quality requirements to further reject charged hadrons and electrons from photon conversions [17]. A set of cuts on these discriminating variables are identified to maximize the background rejection while keeping a high electron signal efficiency. Such

cuts are determined for different pseudorapidity and E_{T} regions to maintain a high electron efficiency across the detector and over the electron transverse energy range. The selection of $Z\gamma$ events requires two oppositely charged "medium" electrons with $E_{\mathrm{T}} > 20$ GeV. For the $W\gamma$ selection one "tight" electron is required in the event with $E_{\mathrm{T}} > 20$ GeV. The event is rejected if there is an additional "medium" electron candidate present that passes the same kinematic cuts.

The photon candidates use clustered energy deposits in the EM calorimeter in the range $|\eta| < 2.37$ (excluding the region $1.37 < |\eta| < 1.52$) and with $E_{\mathrm{T}} > 15$ GeV. As for electrons, the photon identification is based on discriminating variables computed from calorimeter information which provides a good separation of signal from background. In particular the high granularity of the first (strip) layer in the η direction that covers up to $|\eta| < 2.4$, provides a very effective discrimination between single photon and multiple-photon showers produced in meson (e.g. π^0, η) decays. A set of cuts on these discriminating variables is identified for different pseudorapidity regions. The cuts are applied separately for converted and unconverted photons to account for the wider shower shapes of the former due to the opposite bending of the two legs from the conversion in the solenoid magnetic field. To further reduce the background due to photons from π^0 and η decays, an isolation requirement of $E_{\mathrm{T}}^{\mathrm{iso}} < 5$ GeV is applied. $E_{\mathrm{T}}^{\mathrm{iso}}$ is the total transverse energy recorded in the calorimeter (of both electromagnetic and hadronic systems) in a cone of radius $\Delta R = 0.4$ around the photon direction (excluding a small window of 0.125×0.175 in the $\eta - \phi$ space which contains the photon energy deposit). $E_{\mathrm{T}}^{\mathrm{iso}}$ is corrected for the leakage of the photon energy into the isolation cone and the contributions from the underlying and pile-up activities in the event [18].

The reconstruction of the missing transverse energy ($E_{\mathrm{T}}^{\mathrm{miss}}$) follows the definition in Ref. [17]. The $E_{\mathrm{T}}^{\mathrm{miss}}$ calculation is based on the energy deposits of calorimeter cells inside three-dimensional clusters. Corrections for hadronic to electromagnetic energy scale, dead material, out-of-cluster energy as well as muon momentum for the muon channel are applied. Events that have sporadic calorimeter noise and non-collision backgrounds, which can affect the $E_{\mathrm{T}}^{\mathrm{miss}}$ reconstruction, are removed [20].

5.2 Event Selection

In addition to the presence of one high p_{T} lepton and one high E_{T} isolated photon, $W\gamma$ candidates are required to have $E_{\mathrm{T}}^{\mathrm{miss}} > 25$ GeV and the transverse mass of the lepton-$E_{\mathrm{T}}^{\mathrm{miss}}$ system $m_{\mathrm{T}}(l,\nu) > 40$ GeV, where $m_{\mathrm{T}}(l,\nu) = \sqrt{2p_{\mathrm{T}}(l) \cdot E_{\mathrm{T}}^{\mathrm{miss}} \cdot (1 - \cos\Delta\phi)}$, and $\Delta\phi$ is the azimuthal separation between the directions of the lepton and the missing transverse energy vector. For $Z\gamma$ candidates, the invariant mass of the two opposite charged leptons ($m_{l^+l^-}$) is required to be greater than 40 GeV. In both $W\gamma$ and $Z\gamma$ analyses, a $\Delta R(l,\gamma) > 0.7$ cut is applied to suppress the contributions from FSR photons in the W and Z boson decays. A total of 192 $W\gamma$ candidates (95 in the electron and 97 in the muon channel) and 48 $Z\gamma$ candidates (25 in the electron and 23 in the muon channel) pass all the requirements.

5.3 Kinematic Distributions of Event Candidates

The distributions of kinematic variables from the data are compared to signal plus background expectations using the combined electron and muon channels for the selected $W\gamma$ and $Z\gamma$ event candidates. The distributions of the photon E_{T}, ΔR between lepton and photon, the two body transverse mass $m_{\mathrm{T}}(l,\nu)$ and the three body transverse mass $m_{\mathrm{T}}(l,\nu,\gamma)$ of $W\gamma$ candidates are shown in Fig. 3. The three body transverse mass, $m_{\mathrm{T}}(l,\nu,\gamma)$, is defined in Equation (5.1) [10]

$$\begin{aligned} m_{\mathrm{T}}^2(l,\nu,\gamma) = & (\sqrt{M_{l\gamma}^2 + |\vec{p}_{\mathrm{T}}(\gamma) + \vec{p}_{\mathrm{T}}(l)|^2} + E_{\mathrm{T}}^{\mathrm{miss}})^2 \\ & -|\vec{p}_{\mathrm{T}}(\gamma) + \vec{p}_{\mathrm{T}}(l) + \vec{E}_{\mathrm{T}}^{\mathrm{miss}}|^2 \end{aligned} \tag{5.1}$$

where $M_{l\gamma}$ is the invariant mass of the lepton-photon system. In the photon distribution (Fig. 3a) the data show a slight excess over expectation at high E_{T}^{γ}. However the excess is not significant as there are 9 observed events for $E_{\mathrm{T}}^{\gamma} > 85$ GeV and we expect about 5 events.

The distributions of the three body invariant mass $m_{l^+l^-\gamma}$ and the two-dimensional plots of $m_{l^+l^-\gamma}$ vs $m_{l^+l^-}$ for the $Z\gamma$ candidates are shown in Fig. 4. The data points are compared to the sum of the NLO SM predictions for the $W\gamma$ and $Z\gamma$ plus the various background contributions. All backgrounds, except the W+jets for the $W\gamma$ analysis, are estimated from simulation and normalized with the predicted NLO cross section values. For the W+jets contribution, the shape of the background is taken from simulations while the absolute normalization is determined from a data-driven method described in Section 7.

6 Efficiency Estimation

6.1 Trigger Efficiency

The performance of the electron high p_{T} trigger has been measured with data and found to be 99±1% efficient for both "medium" and "tight" electrons with $E_{\mathrm{T}} > 20$ GeV, with negligible η and E_{T} dependence [17]. The efficiency of the muon trigger is also measured with data, using $Z \to \mu^+\mu^-$ events [19]. The overall efficiencies to trigger on the $W\gamma$ and $Z\gamma$ events, in the muon decay channel, are $86.2 \pm 0.5\%$ and $97.5 \pm 0.2\%$ respectively. The electron (muon) trigger efficiency is measured with respect to an electron (muon) candidate which has passed the offline selection cuts. The muon trigger efficiency is lower than the electron trigger efficiency due to limited coverage of the trigger chambers.

6.2 Lepton Identification Efficiency

The electron identification efficiency $\varepsilon_e^{\mathrm{ID}}$ is defined as the probability of electrons in signal events reconstructed within the kinematic and geometric requirements to pass the identification quality cuts [17]. The efficiency for the "tight" selection in $W\gamma$ events is 73±4%. For the "medium" selection in $Z\gamma$ events, the efficiency is 92±2% and 87±3% for the leading and sub-leading electron, respectively. These efficiencies are evaluated from signal MC

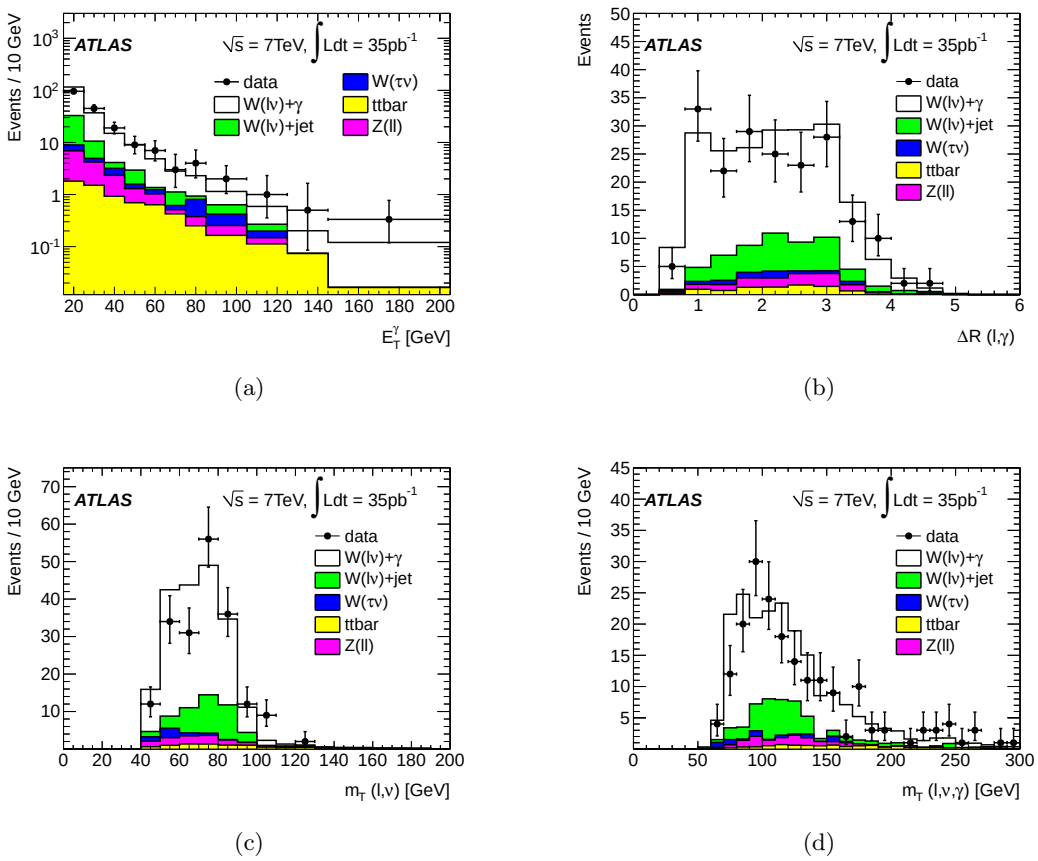

Figure 3. Distributions for the combined electron and muon decay channels of the photon transverse energy (a), ΔR between lepton and photon (b), two body transverse mass ($m_{\mathrm{T}}(l,\nu)$) (c) and three body transverse mass ($m_{\mathrm{T}}(l,\nu,\gamma)$) (d) of the $W\gamma$ candidate events. MC predictions for signal and backgrounds are also shown.

events with scale factors applied to correct for discrepancies with data. The scale factors are obtained by comparing the electron efficiency in MC to an *in situ* electron efficiency measured in data from unbiased probe electrons selected together with a well identified tag electron in $Z \to e^+e^-$ candidate events, and from unbiased probe electrons in selected $W \to e\nu$ candidate events with large and isolated $E_{\mathrm{T}}^{\mathrm{miss}}$ recorded by the $E_{\mathrm{T}}^{\mathrm{miss}}$ trigger. The uncertainties on $\varepsilon_e^{\mathrm{ID}}$ account for background contamination in the unbiased probe electron sample, and the potential bias from tag requirements of the *in situ* efficiency measurement. The results of the two *in situ* efficiency measurements from $Z \to ee$ and $W \to e\nu$ are combined with weights proportional to their uncertainties.

Unbiased muons from $Z \to \mu^+\mu^-$ candidate events are used to cross check the muon identification efficiency $\varepsilon_\mu^{\mathrm{ID}}$ calculated with the MC signal sample [17, 19]. The single muon identification efficiency for the $W\gamma$ and $Z\gamma$ analyses is estimated to be $89 \pm 1\%$. The muon momentum scale and resolution are studied by comparing the mass distribution of $Z \to \mu^+\mu^-$ in data and MC [17]. The uncertainty in the acceptance of the $W\gamma$ ($Z\gamma$)

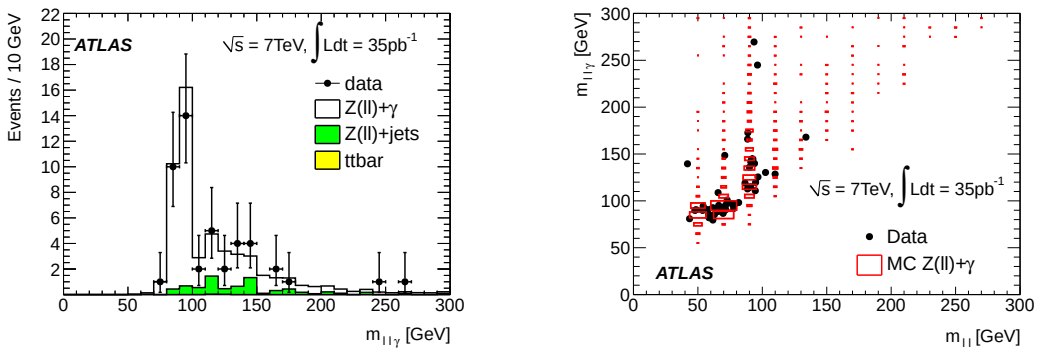

(a) (b)

Figure 4. (a) Three body invariant mass $m_{l^+l^-\gamma}$ distribution for $Z\gamma$ data candidate events. MC predictions for signal and backgrounds are also shown. (b) Two-dimensional plots of $m_{l^+l^-\gamma}$ vs $m_{l^+l^-}$ for $Z\gamma$ data candidate events. The MC signal prediction is also shown. Both the electron and muon decay channels are included.

signal events due to the uncertainties in the corrections of the muon momentum scale and resolution of the MC is $\sim 0.3\%$ ($\sim 0.5\%$).

6.3 Photon Identification Efficiency

The photon identification efficiency, $\varepsilon_\gamma^{\rm ID}$, is defined as the probability of photons in signal events, reconstructed within the kinematic and geometric acceptance to pass the photon identification requirements. The photon identification efficiency is determined from $W\gamma$ and $Z\gamma$ MC samples where the discriminating variable distributions are corrected (by simple shifts) to account for observed discrepancies between data and simulation. Corrections for each discriminating variable are calculated separately for photons in the range $|\eta| < 1.8$ and $|\eta| > 1.8$. This separation is motivated by the significantly larger discrepancies observed in the high pseudorapidity region where the amount of material in front of the calorimeter is known less well. The data/simulation corrections are determined by comparing the discriminating variable distributions for photons in signal MC samples and candidate photons in $W\gamma$ data events (before the isolation requirement). The impact of the corrections on the photon identification efficiency is -3% (-5%) resulting in an estimated $\varepsilon_\gamma^{\rm ID}$ of 71% (67%) for photons in the range $|\eta| < 1.8$ ($|\eta| > 1.8$). The main source of systematic uncertainty comes from the knowledge of the upstream material. A dedicated simulated sample that includes additional material in the inner detector and in front of the electromagnetic calorimeter was used to assess the impact of a different account of material budget on the photon identification efficiency. The resulting uncertainty on $\varepsilon_\gamma^{\rm ID}$ is 6.3% (7.5%) for photons in the range $|\eta| < 1.8$ ($|\eta| > 1.8$). Other sources of uncertainty arise from the simple shift approximation for the data/simulation corrections (3%), from the discriminating variable distribution bias due to background contamination in the $W\gamma$ photon candidate data sample (4%), and from inefficiencies in the reconstruction of photon conversions (2%). Since only prompt photons are present in the $W\gamma$ and $Z\gamma$ MC samples,

the efficiency of the fragmentation photon component is calculated using an ALPGEN [21] "$W+1$ jet" fully simulated sample by selecting events with a high E_{T} photon produced in the jet fragmentation. The fractional contribution of fragmentation photons to the total cross section is estimated by the Baur NLO generator (see Section 1) to be 8%. Since there is a large uncertainty on the fragmentation photon contribution to the $W\gamma$ and $Z\gamma$ cross sections, a conservative error of 100% is considered on such an estimate which leads to an additional 3% uncertainty on the photon identification efficiency.

Taking into account all the contributions, the overall uncertainty on the photon reconstruction and identification efficiency is then estimated to be 10.2% (13.0%) for photons in the range $|\eta| < 1.8$ ($|\eta| > 1.8$).

6.4 Photon Isolation Efficiency

The efficiency, $\varepsilon_{\gamma}^{\mathrm{iso}}$, of the photon isolation requirement is estimated with the signal $W\gamma$ and $Z\gamma$ MC and cross checked with data using electrons from the $Z \to e^{+}e^{-}$ sample (after taking into account the differences between the electromagnetic showering of electrons and photons). The resulting photon isolation efficiency, within its systematic uncertainty, is found to be consistent with the one derived from the signal MC. The systematic uncertainties for $\varepsilon_{\gamma}^{\mathrm{iso}}$ are due to the background contamination in the electron sample (1%), the shape differences of the $E_{\mathrm{T}}^{\mathrm{iso}}$ distribution between electrons and photons (0.6%), and the differences in p_{T} spectrum between electrons and photons (1.5%). As for the photon identification efficiency, the $\varepsilon_{\gamma}^{\mathrm{iso}}$ for the fragmentation components is obtained from an ALPGEN "$W+1$ jet" fully simulated sample and an additional 3% uncertainty is quoted to account for the uncertainty on the fragmentation photon contribution. The overall $\varepsilon_{\gamma}^{\mathrm{iso}}$ is 95% with a total estimated uncertainty of 3.3%.

7 Background Determination and Signal Yield

The dominant sources of background for this analysis are from $W(Z)$+jets events where photons from the decay products of mesons produced by the jet fragmentation (mainly $\pi^{0} \to \gamma\gamma$) pass the photon selection criteria. Since the fragmentation functions of quarks and gluons into hadrons are poorly constrained by experiments, these processes are not well modeled by W+jets MC simulations. For the $W\gamma$ analysis the amount of this background is estimated from ATLAS data while for the $Z\gamma$ analysis, due to the limited statistics, a MC based estimation is performed and a large uncertainty of 100% is assigned. Additional backgrounds from other processes, such as $W \to \tau\nu$, $t\bar{t}$, and $Z \to e^{+}e^{-}(\mu^{+}\mu^{-})$ (misidentified as $W\gamma$) for the $W\gamma$ analysis, and $t\bar{t}$ and Z+jets for the $Z\gamma$ analysis will be referred to collectively as "EW+$t\bar{t}$ background" and their contribution is estimated from MC simulation.

The background from mesons decaying to photons is determined directly from the selected $W\gamma$ events using a two-dimensional sideband method. This allows the extraction of the $W\gamma$ signal yield directly from data. Although currently limited in statistics, this method is preferred over use of average photon background estimates from high statistics jet trigger data samples because of the very different probability for gluon and quark

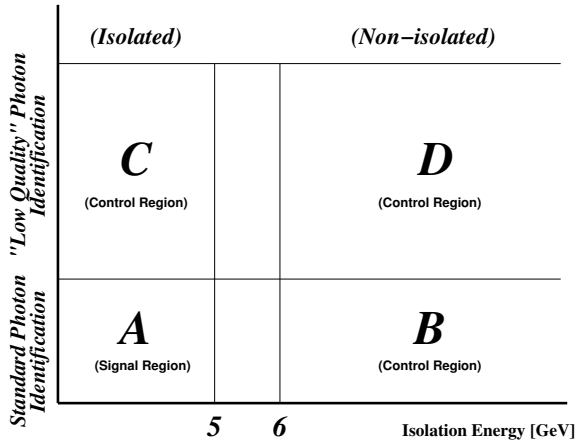

Figure 5. Sketch of the two-dimensional plane defining the 4 regions used in the sideband method. Region A is the signal region. The non-isolated control regions (B and D) are defined for photons with $E_{\mathrm{T}}^{\mathrm{iso}} > 6$ GeV. The "low quality photon identification" control regions (C and D) include photons passing all the identification criteria except the strip layer discriminating variable requirements (see Section 5.1).

initiated jets to pass the photon identification criteria (estimated to be different by one order of magnitude [22]), and the poor knowledge of the quark to gluon ratio between jets in W+jets events and generic inclusive jet production.

The two variables used for the sideband method are $E_{\mathrm{T}}^{\mathrm{iso}}$ and the identification "quality" of the photon candidate. Three control regions are defined to estimate the amount of W+jets background in the signal region (see Fig. 5). The signal yield of the selected $W\gamma$ sample is extracted by simply subtracting from the number of candidate events the amount of background in the signal region N_{A}. This can be determined by studying the background in the three control regions with the assumption that for the background the ratio of isolated to non-isolated events in the sample passing the photon identification criteria ($N_{\mathrm{B}}/N_{\mathrm{A}}$) is the same as in the sample passing the "low quality" identification criteria ($N_{\mathrm{D}}/N_{\mathrm{C}}$). Finally the backgrounds in the control regions are taken directly from the number of observed events in data. Corrections are applied to subtract the contribution in these regions from signal events (estimated from MC to be around 10% in region C, few percent in region B, and to be negligible in region D) and the contribution from "EW+$t\bar{t}$ background" (of the order of 10% in all three regions).

The W+jets background contribution as estimated by this data-driven method is reported in Table 1. In the same table the estimated $W\gamma$ signal yield as well as the total background and signal yield for the $Z\gamma$ analysis are shown. The effective purity, P, of the $W\gamma$ ($Z\gamma$) sample, defined as the fraction of signal in the selected events (after the subtraction of the "EW+$t\bar{t}$ background" contribution), is calculated to be around 80% (85%).

The accuracy of the W+jets background determination with the two-dimensional sideband method has been carefully assessed. The uncertainty related to the definition of the control regions is determined by studying the impact of possible variations of their defini-

Process	Observed events	EW+$t\bar{t}$ background	W+jets background	Extracted signal
$N_{obs}(W\gamma \to e^{\pm}\nu\gamma)$	95	$10.3 \pm 0.9 \pm 0.7$	$16.9 \pm 5.3 \pm 7.3$	$67.8 \pm 9.2 \pm 7.3$
$N_{obs}(W\gamma \to \mu^{\pm}\nu\gamma)$	97	$11.9 \pm 0.8 \pm 0.8$	$16.9 \pm 5.3 \pm 7.4$	$68.2 \pm 9.3 \pm 7.4$
Process	Observed events	EW+$t\bar{t}$ background		Extracted signal
$N_{obs}(Z\gamma \to e^{+}e^{-}\gamma)$	25	3.7 ± 3.7		$21.3 \pm 5.8 \pm 3.7$
$N_{obs}(Z\gamma \to \mu^{+}\mu^{-}\gamma)$	23	3.3 ± 3.3		$19.7 \pm 4.8 \pm 3.3$

Table 1. Numbers of the total observed candidate events, estimated number of background and estimated number of signal events for the $pp \to l^{\pm}\nu\gamma + X$ and $pp \to l^{+}l^{-}\gamma + X$ selected samples. Where two uncertainties are quoted the first is statistical and the second represents an estimate of systematics. Statistical errors in MC predictions are treated as a systematic in the propagation of uncertainties on the W+jets background and the extracted signal. The W+jets background contribution is estimated from ATLAS data with a two-dimensional sideband method. For the $pp \to l^{+}l^{-}\gamma + X$ process the uncertainty on the MC based background estimate is 100%.

tions. For the non-isolated control regions (B and D) the lower boundary of 6 GeV has been shifted by ± 1 GeV, probing different mixtures of background and $W\gamma$ signal event contamination. For the "low quality" photon identification control regions (C and D) two alternative choices of strip layer discriminating variable criteria are tested. These changes of control region definitions lead to respectively a 4% and a 9% variation of the effective purity estimate. The contamination from $W\gamma$ signal events in the control regions is strongly correlated with the photon identification efficiency in the signal region (an overestimate of the latter induces an underestimate of the former). Shifting the discriminating variable distributions of the signal MC in a way similar to the one described in Section 6.3 results in an impact on the effective purity estimation of the order of 3%. Finally, the accuracy on the assumption that the correlations between the two-dimension variables (namely the energy isolation and the photon identification quantities) are negligible for background events has been evaluated by applying the same method to background samples extracted from W+jets MC events. The corresponding purities are all found to be compatible with zero and their values are used to determine the systematic uncertainty associated to the method, estimated to be 3%. For the "EW+$t\bar{t}$ background" estimation, the corresponding NLO theoretical cross section uncertainty (between 6% to 7% depending on the process) and the luminosity uncertainty (3.4%) are used.

In Fig. 6a (6b), the $E_{\mathrm{T}}^{\mathrm{iso}}$ distribution of photon candidate events in the $W\gamma$ ($Z\gamma$) combined sample is shown along with the predicted contributions for the background.

8 Cross Section Measurements and Comparison to Theoretical Calculations

8.1 Fiducial cross section measurement for $W\gamma$ and $Z\gamma$

The measurements for the fiducial cross sections for the processes $pp \to l^{\pm}\nu\gamma + X$ and $pp \to l^{+}l^{-}\gamma + X$ can be expressed as

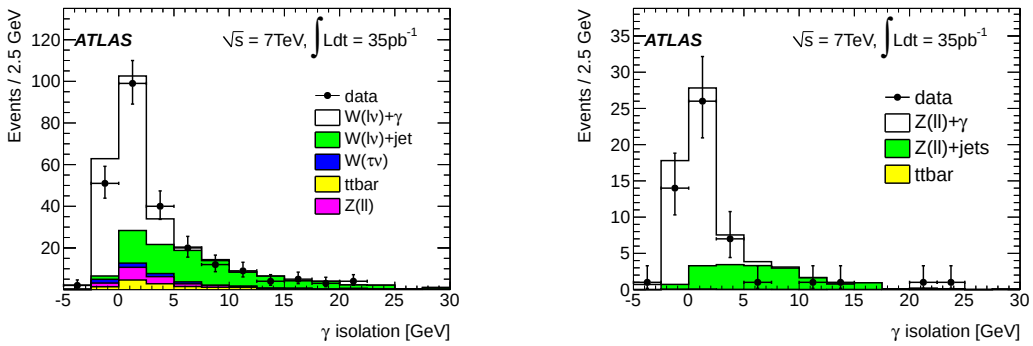

(a) (b)

Figure 6. Photon isolation distribution for photon candidates in the $W\gamma$ (a) and in the $Z\gamma$ (b) data events (points). The shape of the predicted W+jets background is taken from the data photon isolation distribution of events in the control regions C-D while the normalization is determined by the two-dimensional sideband data-driven method. The predicted contributions from the other backgrounds and from the signal are taken from MC.

$$\sigma^{\text{fid}}_{pp\to l^{\pm}\nu\gamma(l^{+}l^{-}\gamma)} = \frac{N^{\text{sig}}_{W\gamma(Z\gamma)}}{C_{W\gamma(Z\gamma)} \cdot L_{W\gamma(Z\gamma)}} \tag{8.1}$$

where

- $N^{\text{sig}}_{W\gamma}$ and $N^{\text{sig}}_{Z\gamma}$ denote the number of background-subtracted signal events passing the selection criteria of the analyses in the $W\gamma$ and $Z\gamma$ channels. The N^{sig} values for both $W\gamma$ and $Z\gamma$ processes are given in Table 1.
- $L_{W\gamma}$ and $L_{Z\gamma}$ denote the integrated luminosities for the channels of interest.
- $C_{W\gamma}$ and $C_{Z\gamma}$ are correction factors and denote the probability for events generated within the fiducial region of the phase-space (as defined in Table 2) to pass the final selection requirements.

The correction factors $C_{W\gamma(Z\gamma)}$ include all trigger efficiencies, selection efficiencies and reconstruction efficiencies of the photon and leptons.

$$C_{W\gamma} = \varepsilon^{W\gamma}_{\text{event}} \cdot \varepsilon^{\text{ID}}_{\text{lep}} \cdot \varepsilon^{W\gamma}_{\text{trig}} \cdot \varepsilon^{\text{ID}}_{\gamma} \cdot \varepsilon^{\text{iso}}_{\gamma} \cdot \alpha^{W\gamma}_{\text{reco}} \tag{8.2}$$

$$C_{Z\gamma} = \varepsilon^{Z\gamma}_{\text{event}} \cdot (\varepsilon^{\text{ID}}_{\text{lep}})^2 \cdot \varepsilon^{Z\gamma}_{\text{trig}} \cdot \varepsilon^{\text{ID}}_{\gamma} \cdot \varepsilon^{\text{iso}}_{\gamma} \cdot \alpha^{Z\gamma}_{\text{reco}} \tag{8.3}$$

where

- $\varepsilon^{W\gamma}_{\text{trig}}$ and $\varepsilon^{Z\gamma}_{\text{trig}}$ denote the probability of $W\gamma$ and $Z\gamma$ events to be recorded by the electron or muon trigger.
- $\varepsilon^{W\gamma}_{\text{event}}$ and $\varepsilon^{Z\gamma}_{\text{event}}$ denote event selection efficiencies (including efficiency of primary vertex requirement).

Fiducial phase space				
	$e^{\pm}\nu\gamma$	$e^{+}e^{-}\gamma$	$\mu^{\pm}\nu\gamma$	$\mu^{+}\mu^{-}\gamma$
$E_{\mathrm{T}}^{l}(p_{\mathrm{T}}^{l})$	$E_{\mathrm{T}}^{e} > 20$ GeV $p_{\mathrm{T}}^{\nu} > 25$ GeV	$E_{\mathrm{T}}^{e} > 20$ GeV -	$p_{\mathrm{T}}^{\mu} > 20$ GeV $p_{\mathrm{T}}^{\nu} > 25$ GeV	$p_{\mathrm{T}}^{\mu} > 20$ GeV -
η_l	$0 < \lvert\eta_e\rvert < 1.37$ or $1.52 < \lvert\eta_e\rvert < 2.47$	$0 < \lvert\eta_e\rvert < 1.37$ or $1.52 < \lvert\eta_e\rvert < 2.47$	$\lvert\eta_\mu\rvert < 2.4$	$\lvert\eta_\mu\rvert < 2.4$
Boson cut	$m_{\mathrm{T}} > 40$ GeV	$m_{ee} > 40$ GeV	$m_{\mathrm{T}} > 40$ GeV	$m_{\mu\mu} > 40$ GeV
Photon	$E_{\mathrm{T}}^{\gamma} > 15$ GeV $0 < \lvert\eta_\gamma\rvert < 1.37$ or $1.52 < \lvert\eta_\gamma\rvert < 2.37$ $\Delta R(l,\gamma) > 0.7$ $\epsilon_h^p < 0.5$			
Phase space for production cross section				
	$e^{\pm}\nu\gamma$	$e^{+}e^{-}\gamma$	$\mu^{\pm}\nu\gamma$	$\mu^{+}\mu^{-}\gamma$
Boson		$m_{ee} > 40$ GeV		$m_{\mu\mu} > 40$ GeV
Photon	$E_{\mathrm{T}}^{\gamma} > 15$ GeV $\Delta R(l,\gamma) > 0.7$ $\epsilon_h^p < 0.5$			

Table 2. Definition of the fiducial phase space at the particle level, where the measurements are performed and the extended phase space (common to all measurements), where the production cross sections are evaluated. ϵ_h^p is defined in Section 2.

- $\varepsilon_{\mathrm{lep}}^{\mathrm{ID}}$ denotes lepton identification efficiency.
- $\varepsilon_{\gamma}^{\mathrm{ID}}$ denotes photon identification efficiency.
- $\varepsilon_{\gamma}^{\mathrm{iso}}$ denotes photon isolation efficiency.
- $\alpha_{\mathrm{reco}}^{W\gamma}$ and $\alpha_{\mathrm{reco}}^{Z\gamma}$ account for all differences observed between the efficiencies of applying the kinematic and geometrical cuts at generator level and reconstruction level. Their values are not closed to 100% mainly due to acceptance loss of the electron and photon reconstruction caused by some inoperative readouts in the electromagnetic calorimeter, reconstruction efficiencies of the leptons and photon, and the detector resolution on the lepton transverse momenta/energies and on the missing transverse energy.

The central values of the correction factors $C_{W\gamma}$ and $C_{Z\gamma}$ are computed using $W\gamma$ and $Z\gamma$ signal MC samples, with scale factor corrections to account for discrepancies in trigger, lepton and photon selection efficiencies between data and MC, as described in Section 6. The central values of the correction factors $C_{W\gamma}$ ($C_{Z\gamma}$) of both electron and muon channels together with their components are given in Table 3.

The breakdown of the uncertainties on $C_{W\gamma}$ and $C_{Z\gamma}$ is reported in Table 4 and 5. The uncertainties related to the efficiency components of $C_{W\gamma}$ and $C_{Z\gamma}$ have been discussed in Section 6. Other sources of uncertainties include:

- The impact of the EM energy scale uncertainty is evaluated by propagating the EM energy scale uncertainties to the number of accepted $W\gamma$ and $Z\gamma$ events. The EM energy scale uncertainty, after applying *in situ* data driven calibration to correct for cluster energies of photon and electron clusters, is quoted to be 1% in the barrel region, and 3% in the endcap region.

- The muon momentum scale and resolution are studied by comparing the mass distribution of $Z \to \mu^+\mu^-$ in data and MC simulations [17]. The uncertainty in the acceptance of the $W\gamma$ ($Z\gamma$) signal events due to the uncertainties in the corrections of the muon momentum scale and resolution of the MC simulations is $\sim 0.3\%$ ($\sim 0.5\%$).

- The acceptance loss from a few inoperative optical links of the calorimeter readout is evaluated from the signal MC. The imperfect modeling of this acceptance loss need to be considered in the systematics uncertainty of $C_{W\gamma}$ and $C_{Z\gamma}$. This uncertainty is estimated to be about 0.7% for a single (e/γ) object.

- The experimental uncertainty arising from the transport of low-energy bremsstrahlung photons through the detector material and the response of the electromagnetic calorimeter is estimated to be less than 0.3% [17].

- The main uncertainty on the scale of the missing transverse energy is determined from a variation of the response of cells in topological clusters. Other sources of uncertainty, namely the imperfect modelling of the overall $E_{\mathrm{T}}^{\mathrm{miss}}$ response (e.g. from low energy hadrons) and resolution, of the underlying event and pile-up effects are also considered. The overall impact on $C_{W\gamma}$ is 2% [17].

All the quantities needed to calculate the cross sections defined in Equation (8.1), along with their uncertainties, are tabulated in Table 6. Using these numbers, the measured fiducial cross sections for the $pp \to l^{\pm}\nu\gamma + X$ and $pp \to l^+l^-\gamma + X$ processes are determined. The results are presented in Table 7 and also illustrated in Fig. 7. MC statistical uncertainties are included as part of the cross sections systematics. The most significant systematic uncertainties in both measurements arise from the background estimation and the efficiencies of photon identification and isolation.

8.2 Production Cross Section Measurement for $W\gamma$ and $Z\gamma$

The production cross sections for the $W\gamma$ and $Z\gamma$ processes are defined for the full decay phase space of the W and Z bosons and for photons with $E_{\mathrm{T}}^{\gamma} > 15$ GeV, $\Delta R(l,\gamma) > 0.7$ and $\epsilon_h^p < 0.5$. These cross sections can be derived from fiducial cross sections by extrapolation from the fiducial phase space to the extended phase space, where production cross sections are defined. The definition of the production cross sections is shown in Equation (8.4).

$$\sigma_{pp\to l^{\pm}\nu\gamma(pp\to l^+l^-\gamma)} = \frac{\sigma^{\mathrm{fid}}_{pp\to l^{\pm}\nu\gamma(pp\to l^+l^-\gamma)}}{A_{W\gamma(Z\gamma)}} \tag{8.4}$$

	$pp \to e^{\pm}\nu\gamma$	$pp \to \mu^{\pm}\nu\gamma$	$pp \to e^{+}e^{-}\gamma$	$pp \to \mu^{+}\mu^{-}\gamma$
$\varepsilon_{\text{event}}$	100%	100%	100%	100%
$\varepsilon_{\text{trig}}^{\text{event}}$	99%	86%	100%	98%
$\varepsilon_{\text{lep}}^{\text{ID}}$	73%	89%	90%	88%
$\varepsilon_{\gamma}^{\text{ID}}$	70%	71%	70%	70%
$\varepsilon_{\gamma}^{\text{iso}}$	95%	96%	96%	96%
α_{reco}	75%	87%	53%	85%
$C_{V\gamma}$	36%	46%	28%	43%

Table 3. Efficiency factors per lepton and α_{reco}, which enter the calculation of the correction factors $C_{V\gamma}$ (where V denotes W or Z boson) for both lepton channels. The trigger efficiencies are measured from data. The other efficiencies are determined from MC simulation and have been validated with data, as described in Section 6. A detailed summary of the various contributions entering the uncertainty on $C_{V\gamma}$ is given in Table 4 and 5.

Parameter	$\frac{\delta C_{W\gamma}}{C_{W\gamma}}$	$\frac{\delta C_{Z\gamma}}{C_{Z\gamma}}$	$\delta(\frac{C_{W\gamma}}{C_{Z\gamma}})/\frac{C_{W\gamma}}{C_{Z\gamma}}$
Channel	$e^{\pm}\nu\gamma$	$e^{+}e^{-}\gamma$	Electron
Trigger efficiency	1%	0.02%	1%
Electron efficiency	4.5%	4.5%	4.5%
Photon efficiency	10.1%	10.1%	-
EM scale and resolution	3%	4.5%	1.5%
$E_{\text{T}}^{\text{miss}}$ scale and resolution	2%	-	2%
Inoperative readout modeling	1.4%	2.1%	0.7%
Photon simulation modeling	0.3%	0.3%	0.3%
Photon isolation efficiency	3.3%	3.3%	-
Total uncertainty	12.1%	12.5%	5.3%

Table 4. Summary of the different terms contributing to the uncertainty on $C_{W\gamma}$ and $C_{Z\gamma}$ for the electron final state. The decomposition has been made such that correlations between the various contributions are negligible.

The acceptance factors $A_{W\gamma}$ and $A_{Z\gamma}$ are defined as the fraction of weighted events in the $W(Z) + \gamma$ LO MC sample, generated within the phase space of the production cross section, that satisfy the geometrical and kinematic constraints of the fiducial cross section as shown in Table 2. The weight of the LO MC events is from QCD NLO correction k-factors, which also include contributions from fragmentation components as described in section 2.

The systematic uncertainties on the acceptances are dominated by the limited knowledge of the proton PDFs. These are evaluated by comparing the acceptances obtained by adopting different PDF sets (including CTEQ6L1 [8], HERAPDF1.0 [23] and MRST LO* [24]). Other contributions are the uncertainties due to the NLO correction of $W\gamma$ and $Z\gamma$ production, which is derived from the difference between the Born level acceptance and acceptance in Baur NLO simulations. The overall relative systematic uncertainty on $A_{W\gamma}$ ($A_{Z\gamma}$) is 4.5% (6.7%), the relative systematic uncertainty for the $A_{W\gamma}/A_{Z\gamma}$ ratio is 4%.

Parameter	$\frac{\delta C_{W\gamma}}{C_{W\gamma}}$	$\frac{\delta C_{Z\gamma}}{C_{Z\gamma}}$	$\delta(\frac{C_{W\gamma}}{C_{Z\gamma}})/\frac{C_{W\gamma}}{C_{Z\gamma}}$
Channel	$\mu^{\pm}\nu\gamma$	$\mu^{+}\mu^{-}\gamma$	Muon
Trigger efficiency	0.6%	0.2%	0.6%
Muon efficiency	0.5%	1%	0.5%
Muon isolation efficiency	1%	2%	1%
Momentum scale and resolution	0.3%	0.5%	0.2%
Photon efficiency	10.1%	10.1%	-
EM scale and resolution	4%	3%	1%
$E_{\mathrm{T}}^{\mathrm{miss}}$ scale and resolution	2%	-	2%
Inoperative readout modeling	0.7%	0.7%	-
Photon simulation modeling	0.3%	0.3%	0.3%
Photon isolation efficiency	3.3%	3.3%	-
Total uncertainty	11.6%	11.2%	2.6%

Table 5. Summary of the different terms contributing to the uncertainty on $C_{W\gamma}$ and $C_{Z\gamma}$ for the muon final state. The decomposition has been made such that correlations between the various contributions are negligible.

The measured production cross sections for the $pp \to e^{\pm}\nu\gamma + X$, $pp \to \mu^{\pm}\nu\gamma + X$, $pp \to e^{+}e^{-}\gamma + X$ and $pp \to \mu^{+}\mu^{-}\gamma + X$ processes are summarized in Table 7.

Assuming lepton universality for the W and Z-boson decays, the measured cross sections in the two channels can be combined to reduce the statistical uncertainty. The combination of electron and muon channels in the production cross section measurement is based on the assumption that the uncertainties on the integrated luminosity, on the acceptance correction factors, on the background estimation, and on photon reconstruction, identification, and isolation efficiency are fully correlated. All systematic uncertainties related to lepton efficiencies (i.e. trigger and lepton identification efficiencies) are uncorrelated. The resulting total cross sections for $pp \to l^{\pm}\nu\gamma + X$ and $pp \to l^{+}l^{-}\gamma + X$ processes using the combined electron and muon channels are summarized in Table 7 and plotted in Fig. 7 with a comparison to SM predictions.

8.3 The Ratio of the $W\gamma$ to $Z\gamma$ Cross Sections

The ratio of the $W\gamma$ to $Z\gamma$ cross sections, as defined in Equation (8.5), can be measured with a higher relative precision than the individual cross sections since both experimental and theoretical uncertainties partially cancel. This ratio is a test of the $WW\gamma$ triple gauge coupling predicted by the SM.

$$R = \frac{\sigma_{pp\to l^{\pm}\nu\gamma}}{\sigma_{pp\to l^{+}l^{-}\gamma}} \tag{8.5}$$

In terms of the experimental quantities defined in the previous sections, the ratio R can be written as:

$$R = \frac{N_{W\gamma}^{\mathrm{sig}}}{N_{Z\gamma}^{\mathrm{sig}}} \cdot \frac{C_{Z\gamma}}{C_{W\gamma}} \cdot \frac{A_{Z\gamma}}{A_{W\gamma}} \tag{8.6}$$

	Central value	Statistical uncertainty	Systematic uncertainty	Luminosity uncertainty
	$pp \to e^{\pm}\nu\gamma$			
$N^{\text{sig}}_{W\gamma}$	67.8	9.2	7.3	-
$L_{W\gamma}[\text{pb}^{-1}]$	35.1	-	-	1.2
$C_{W\gamma}$	0.359	0.010	0.043	-
$A_{W\gamma}$	0.131	0.001	0.006	-
	$pp \to e^{+}e^{-}\gamma$			
$N^{\text{sig}}_{Z\gamma}$	21.3	5.8	3.7	-
$L_{Z\gamma}[\text{pb}^{-1}]$	35.1	-	-	1.2
$C_{Z\gamma}$	0.280	0.010	0.035	-
$A_{Z\gamma}$	0.220	0.002	0.015	-
	$pp \to \mu^{\pm}\nu\gamma$			
$N^{\text{sig}}_{W\gamma}$	68.2	9.3	7.4	-
$L_{W\gamma}[\text{pb}^{-1}]$	33.9	-	-	1.2
$C_{W\gamma}$	0.455	0.010	0.053	-
$A_{W\gamma}$	0.134	0.001	0.006	-
	$pp \to \mu^{+}\mu^{-}\gamma$			
$N^{\text{sig}}_{Z\gamma}$	19.7	4.8	3.3	-
$L_{Z\gamma}[\text{pb}^{-1}]$	33.9	-	-	1.2
$C_{Z\gamma}$	0.429	0.010	0.048	-
$A_{Z\gamma}$	0.242	0.002	0.016	-

Table 6. Summary of input quantities for the calculation of the $W\gamma$ and $Z\gamma$ fiducial and production cross sections. For each channel, the observed numbers of signal events after background subtraction, the correction factors $C_{W\gamma(Z\gamma)}$, the acceptance factors $A_{W\gamma(Z\gamma)}$ (see Section 8.2), and the integrated luminosities are given, with their statistical, systematic, and luminosity uncertainties. For $C_{W\gamma(Z\gamma)}$ and $A_{W\gamma(Z\gamma)}$, the statistical uncertainty reflects the limited statistic of the signal MC samples.

The uncertainty on the ratio of the correction factors $\frac{C_{Z\gamma}}{C_{W\gamma}}$ is evaluated separately for the electron and the muon channels, as shown in Table 4 and 5. The uncertainties on the ratio of the acceptance factors $\frac{A_{Z\gamma}}{A_{W\gamma}}$ have already been discussed in Section 8.2. The uncertainties on $N^{\text{sig}}_{W\gamma}$ and $N^{\text{sig}}_{Z\gamma}$, as shown in Table 1, are considered as uncorrelated in the ratio measurement. The measured ratios R in the fiducial phase space and in the total phase space are shown in Table 8 and also illustrated in Fig. 8.

8.4 Comparison to Theoretical Calculation

The Standard Model predictions for the $W\gamma$ and $Z\gamma$ fiducial and production cross sections (as defined in Section 8.1) are given in Table 7. The uncertainty on the cross section predictions includes the following:

- The PDF uncertainty is estimated using the MSTW 08 NLO PDF error eigenvectors [25] at the 90% C.L. limit, and variations of α_s in the range from 0.1145 to 0.1176.

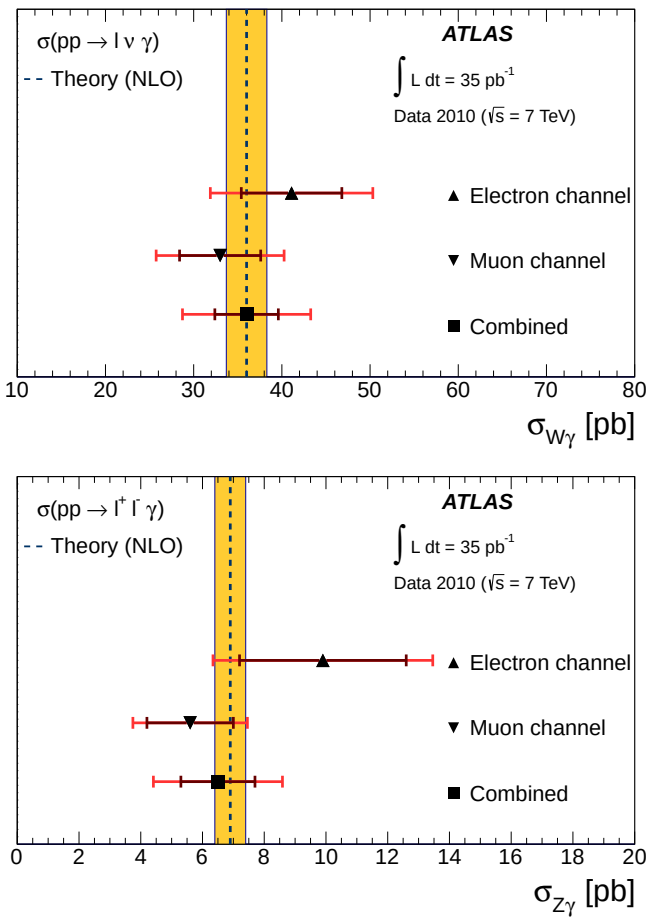

Figure 7. The measured inclusive $W\gamma$ and $Z\gamma$ production cross sections together with SM prediction. Results are shown for the electron and muon final states as well as for their combination. The inner error bar represents the statistical uncertainties and the outer represents the total uncertainties (statistical, systematic and luminosity). All uncertainties are added in quadrature. The one standard deviation uncertainty in the SM prediction is represented by the vertical band.

- Renormalisation and factorisation scale uncertainty: this uncertainty is estimated by varying the renormalisation and factorisation scale by factors of two around the nominal scales.

- An additional 3% error is included to account for the approximation of using the W/Z inclusive k-factor k_{FSR} for the $W(Z)\gamma$.

- Another source of uncertainty accounts for the possible discrepancy between the photon isolation at the particle level and at the parton level. Photon isolation at the parton level (ϵ_h), which is implemented in the Baur NLO program as introduced in Section 4, is used in the calculation of the Standard Model production cross section predictions. The photon isolation criteria at the particle level (ϵ_h^p) is used in the acceptance calculation. This uncertainty is estimated to be 4% by studying the

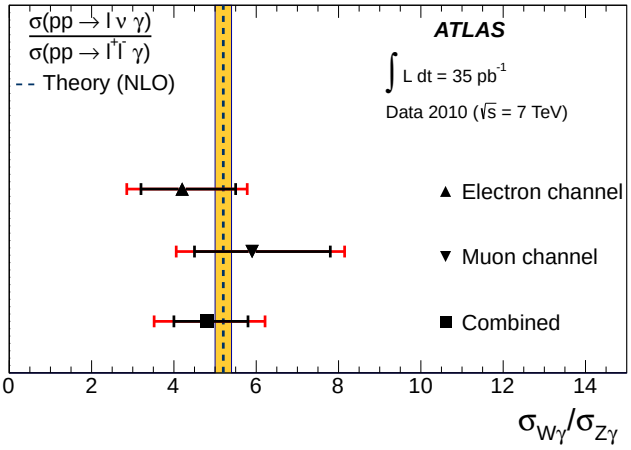

Figure 8. The measured ratio of the production cross sections of $W\gamma$ and $Z\gamma$, together with SM prediction. Results are shown for the electron and muon final states as well as for their combination. The error bars represent the statistical and the total uncertainties. All uncertainties are added in quadrature. The one standard deviation uncertainty in the SM prediction is represented by the vertical band.

impact on the cross section predicted by the Baur NLO generator of a 100% variation of the ϵ_h parameter.

The measured and predicted fiducial and production cross sections of the $pp \to l^{\pm}\nu\gamma + X$ and $pp \to l^+l^-\gamma + X$ processes together with their ratio are shown in Table 7 and Table 8.

9 Summary

The production processes $pp \to l^{\pm}\nu\gamma + X$ and $pp \to l^+l^-\gamma + X$ have been studied at $\sqrt{s} = 7$ TeV using ~ 35 pb^{-1} of data collected with the ATLAS detector. The measured fiducial cross sections (defined in the phase-space region where the detector has good acceptance) and the extrapolated production cross sections (for $E_{\mathrm{T}}^{\gamma} > 15$ GeV, $\Delta R(l,\gamma) > 0.7$, and $\epsilon_h^p < 0.5$) for the individual electron, muon and combined decay channels, are presented. The measurements are in agreement with the predictions of the SM at $O(\alpha\alpha_s)$ as shown in Table 7 and Fig. 7. While the current measurements are not strongly sensitive to possible new physics, the distributions of kinematic variables determined from the leptons and photons (Figs. 3 and 4) are consistent with the predictions from the SM in a new kinematic regime, as is the ratio of the $W\gamma/Z\gamma$ cross sections (Fig. 8), which directly depends upon the values of the triple-gauge-couplings in the Standard Model.

Acknowledgements

We gratefully acknowledge the contributions Ulrich Baur made to the theory calculations used in this study. We thank CERN for the very successful operation of the LHC, as well

	Experimental measurement	SM prediction
	σ^{fid}[pb]	σ^{fid}[pb]
$pp \to e^{\pm}\nu\gamma$	$5.4 \pm 0.7 \pm 0.9 \pm 0.2$	4.7 ± 0.3
$pp \to \mu^{\pm}\nu\gamma$	$4.4 \pm 0.6 \pm 0.7 \pm 0.2$	4.9 ± 0.3
$pp \to e^{+}e^{-}\gamma$	$2.2 \pm 0.6 \pm 0.5 \pm 0.1$	1.5 ± 0.1
$pp \to \mu^{+}\mu^{-}\gamma$	$1.4 \pm 0.3 \pm 0.3 \pm 0.1$	1.7 ± 0.1
	σ[pb]	σ[pb]
$pp \to e^{\pm}\nu\gamma$	$41.1 \pm 5.7 \pm 7.1 \pm 1.4$	36.0 ± 2.3
$pp \to \mu^{\pm}\nu\gamma$	$33.0 \pm 4.6 \pm 5.5 \pm 1.1$	36.0 ± 2.3
$pp \to l^{\pm}\nu\gamma$	$36.0 \pm 3.6 \pm 6.2 \pm 1.2$	36.0 ± 2.3
$pp \to e^{+}e^{-}\gamma$	$9.9 \pm 2.7 \pm 2.3 \pm 0.3$	6.9 ± 0.5
$pp \to \mu^{+}\mu^{-}\gamma$	$5.6 \pm 1.4 \pm 1.2 \pm 0.2$	6.9 ± 0.5
$pp \to l^{+}l^{-}\gamma$	$6.5 \pm 1.2 \pm 1.7 \pm 0.2$	6.9 ± 0.5

Table 7. Fiducial and production cross sections of the $pp \to l^{\pm}\nu\gamma + X$ and $pp \to ll\gamma + X$ process at $\sqrt{s} = 7$ TeV. Both the experimental measurements and the SM NLO predictions are given. The production cross sections are measured with $p_T(\gamma) > 15$ GeV, $\Delta R(l,\gamma) > 0.7$ and $\epsilon_h^p < 0.5$, the fiducial cross section is defined in Section 8. For the measurements, the first uncertainty is statistical, the second is systematic and the third is from the luminosity. The uncertainty in the SM prediction is systematic.

Cross section ratio	Experimental measurement	SM prediction
Fiducial phase space		
$\sigma^{\text{fid}}_{pp\to e^{\pm}\nu\gamma}/\sigma^{\text{fid}}_{pp\to e^{+}e^{-}\gamma}$	$2.5^{+0.8}_{-0.6} \pm 0.5$	3.1 ± 0.3
$\sigma^{\text{fid}}_{pp\to \mu^{\pm}\nu\gamma}/\sigma^{\text{fid}}_{pp\to \mu^{+}\mu^{-}\gamma}$	$3.1^{+1.1}_{-0.8} \pm 0.6$	2.9 ± 0.3
Phase space for production cross section		
$\sigma_{pp\to e^{\pm}\nu\gamma}/\sigma_{pp\to e^{+}e^{-}\gamma}$	$4.2^{+1.3}_{-1.0} \pm 0.9$	5.2 ± 0.2
$\sigma_{pp\to \mu^{\pm}\nu\gamma}/\sigma_{pp\to \mu^{+}\mu^{-}\gamma}$	$5.9^{+1.9}_{-1.4} \pm 1.2$	5.2 ± 0.2
$\sigma_{pp\to l^{\pm}\nu\gamma}/\sigma_{pp\to l^{+}l^{-}\gamma}$	$4.8^{+1.0}_{-0.8} \pm 1.0$	5.2 ± 0.2

Table 8. The ratio of $pp \to l^{\pm}\nu\gamma + X$ to $pp \to l^{+}l^{-}\gamma + X$ process at $\sqrt{s} = 7$ TeV. Both the experimental measurement and the SM NLO prediction are given. The production cross sections are measured with $p_{\mathrm{T}}(\gamma) > 15$ GeV, $\Delta R(l,\gamma) > 0.7$ and $\epsilon_h^p < 0.5$, and the fiducial cross section is defined in Table 2. The first uncertainty in the experimental measurement is statistical and the second uncertainty is systematic. Asymmetric errors calculated from Clopper and Pearson intervals [26] are quoted for the statistical uncertainty, due to the low statistics in the $pp \to l^{+}l^{-}\gamma + X$ measurement. The uncertainty in the SM prediction is systematic.

as the support staff from our institutions without whom ATLAS could not be operated efficiently.

We acknowledge the support of ANPCyT, Argentina; YerPhI, Armenia; ARC, Australia; BMWF, Austria; ANAS, Azerbaijan; SSTC, Belarus; CNPq and FAPESP, Brazil; NSERC, NRC and CFI, Canada; CERN; CONICYT, Chile; CAS, MOST and NSFC,

China; COLCIENCIAS, Colombia; MSMT CR, MPO CR and VSC CR, Czech Republic; DNRF, DNSRC and Lundbeck Foundation, Denmark; ARTEMIS, European Union; IN2P3-CNRS, CEA-DSM/IRFU, France; GNAS, Georgia; BMBF, DFG, HGF, MPG and AvH Foundation, Germany; GSRT, Greece; ISF, MINERVA, GIF, DIP and Benoziyo Center, Israel; INFN, Italy; MEXT and JSPS, Japan; CNRST, Morocco; FOM and NWO, Netherlands; RCN, Norway; MNiSW, Poland; GRICES and FCT, Portugal; MERYS (MECTS), Romania; MES of Russia and ROSATOM, Russian Federation; JINR; MSTD, Serbia; MSSR, Slovakia; ARRS and MVZT, Slovenia; DST/NRF, South Africa; MICINN, Spain; SRC and Wallenberg Foundation, Sweden; SER, SNSF and Cantons of Bern and Geneva, Switzerland; NSC, Taiwan; TAEK, Turkey; STFC, the Royal Society and Leverhulme Trust, United Kingdom; DOE and NSF, United States of America.

The crucial computing support from all WLCG partners is acknowledged gratefully, in particular from CERN and the ATLAS Tier-1 facilities at TRIUMF (Canada), NDGF (Denmark, Norway, Sweden), CC-IN2P3 (France), KIT/GridKA (Germany), INFN-CNAF (Italy), NL-T1 (Netherlands), PIC (Spain), ASGC (Taiwan), RAL (UK) and BNL (USA) and in the Tier-2 facilities worldwide.

References

[1] **ATLAS** Collaboration, *The ATLAS Experiment at the CERN Large Hadron Collider*, *JINST* **3** (2008) S08003.

[2] **The CDF** Collaboration, T. Aaltonen *et al.*, *Measurement of $Z\gamma$ Production in $p\bar{p}$ Collisions at $\sqrt{s} = 1.96$ TeV*, *Phys. Rev.* **D82** (2010) 031103, arXiv:1004.1140.

[3] **The D0** Collaboration, V. Abazov *et al.*, *First study of the radiation-amplitude zero in $w\gamma$ production and limits on anomalous $ww\gamma$ couplings at $\sqrt{s} = 1.96$ tev*, *Phys. Rev. Lett.* **100** (2008) 241805.

[4] **CMS** Collaboration, S. Chatrchyan *et. al.*, *Measurement of W-gamma and Z-gamma production in pp collisions at sqrt(s) = 7 TeV*, arXiv:1105.2758.

[5] J. Alwall *et al.*, *Madgraph/madevent v4: The new web generation*, *JHEP* **0709** (2007) 028.

[6] T. Sjöstrand, S. Mrenna, and P. Skands, *PYTHIA 6.4 physics and manual*, hep-ph/0603175.

[7] P. Golonka and Z. Was, *Photos monte carlo: A precision tool for qed corrections in z and w decays*, *Eur. Phys. J.* **C45** (2006) 97–107.

[8] J. Pumplin *et al.*, *New generation of parton distributions with uncertainties from global qcd analysis*, *JHEP* **0207** (2002) 012.

[9] **ATLAS** Collaboration, "ATLAS Monte Carlo tunes for MC09." ATLAS public note: ATL-PHYS-PUB-2010-002, http://cdsweb.cern.ch/record/1247375.

[10] U. Baur, T. Han, and J. Ohnemus, *Qcd corrections to hadronic $w\gamma$ production with nonstandard $ww\gamma$ couplings*, *Phys. Rev.* **D48** (1993) 5140–5161.

[11] J. Ohnemus, *Order-α_s calculations of hadronic $w\gamma$ and $z\gamma$ production*, *Phy. Rev.* **D47** (1991) 940.

[12] P. Aurenche *et al.*, *Recent critical study of photon production in hadronic collisions*, Phys. Rev. **D73** (2006) 094007.

[13] S. Frixione, P. Nason, and C. Oleari, *Matching nlo qcd computations with parton shower simulations: the powheg method*, *JHEP* **11** (2007) 070.

[14] **ATLAS** Collaboration, *The atlas simulation infrastructure*, *Eur. Phys. J.* **C70** (2010) 823–874.

[15] **ATLAS** Collaboration, *Luminosity Determination in pp Collisions at $\sqrt{s} = 7$ TeV Using the ATLAS Detector at the LHC*, *Eur. Phys. J.* **C71** (2011) 1630. ATLAS Collaboration, *Updated Luminosity Determination in pp Collisions at $\sqrt{s} = 7$ TeV using the ATLAS Detector*, ATLAS conference note: ATLAS-CONF-2011-011, http://cdsweb.cern.ch/record/1334563.

[16] **ATLAS** Collaboration, "Updated Luminosity Determination in pp Collisions at $\sqrt{s} = 7$ TeV using the ATLAS Detector." ATLAS conference note: ATLAS-CONF-2011-011, http://cdsweb.cern.ch/record/1334563.

[17] **ATLAS** Collaboration, *Measurement of the $w \to l\nu$ and $z/\gamma* \to ll$ production cross sections in proton-proton collisions at $\sqrt{s} = 7$ TeV with the atlas detector*, *JHEP* **1012** (2010) 060, arXiv:1010.2130.

[18] **ATLAS** Collaboration, *Measurement of the inclusive isolated prompt photon cross section in pp collisions at sqrt(s) = 7 tev with the atlas detector*, *Phys. Rev.* **D83** (2011) 052005, arXiv:1012.4389.

[19] **ATLAS** Collaboration, *Measurement of the production cross section for w-bosons in association with jets in pp collisions at $\sqrt{s} = 7$ TeV with the atlas detector*, *Phys. Lett. B* **698** (2011) 325–345, arXiv:1012.5382.

[20] **ATLAS** Collaboration, "Data-quality requirements and event cleaning for jets and missing transverse energy re-construction with the ATLAS detector in proton-proton collisions at a center-of-mass energy of $\sqrt{s} = 7$ TeV." ATLAS conference note: ATLAS-CONF-2010-038, http://cdsweb.cern.ch/record/1277678.

[21] M. L. Mangano *et al.*, *Alpgen, a generator for hard multiparton processes in hadronic collisions*, *JHEP* **0307** (2003) 001.

[22] **ATLAS** Collaboration, "Expected performance of the atlas experiment - detector, trigger and physics." CERN-OPEN-2008-020.

[23] **The H1 and ZEUS** Collaboration, F. D. Aaron *et al.*, *Combined measurement and qcd analysis of the inclusive $e^{\pm}p$ scattering cross sections at hera*, *JHEP* **1001** (2010) 109.

[24] A. Sherstnev and R. S. Thorne, *Parton distributions for lo generators*, *Eur. Phys. J.* **C55** (2008) 553–575.

[25] A. D. Martin, W. J. Stirling, R. S. Thorne, and G. Watt, *Parton distributions for the lhc*, arXiv/0901.0002.

[26] R. M. Price and D. G. Bonett, *Estimating the ratio of two poisson rates*, *Computational Statistics & Data Analysis* **34** (September, 2000) 345–356.

The ATLAS Collaboration

G. Aad[48], B. Abbott[111], J. Abdallah[11], A.A. Abdelalim[49], A. Abdesselam[118], O. Abdinov[10], B. Abi[112], M. Abolins[88], H. Abramowicz[153], H. Abreu[115], E. Acerbi[89a,89b], B.S. Acharya[164a,164b], D.L. Adams[24], T.N. Addy[56], J. Adelman[175], M. Aderholz[99], S. Adomeit[98], P. Adragna[75], T. Adye[129], S. Aefsky[22], J.A. Aguilar-Saavedra[124b,a], M. Aharrouche[81], S.P. Ahlen[21], F. Ahles[48], A. Ahmad[148], M. Ahsan[40], G. Aielli[133a,133b], T. Akdogan[18a], T.P.A. Åkesson[79], G. Akimoto[155], A.V. Akimov [94], A. Akiyama[67], M.S. Alam[1], M.A. Alam[76], S. Albrand[55], M. Aleksa[29], I.N. Aleksandrov[65], F. Alessandria[89a], C. Alexa[25a], G. Alexander[153], G. Alexandre[49], T. Alexopoulos[9], M. Alhroob[20], M. Aliev[15], G. Alimonti[89a], J. Alison[120], M. Aliyev[10], P.P. Allport[73], S.E. Allwood-Spiers[53], J. Almond[82], A. Aloisio[102a,102b], R. Alon[171], A. Alonso[79], M.G. Alviggi[102a,102b], K. Amako[66], P. Amaral[29], C. Amelung[22], V.V. Ammosov[128], A. Amorim[124a,b], G. Amorós[167], N. Amram[153], C. Anastopoulos[29], N. Andari[115], T. Andeen[34], C.F. Anders[20], K.J. Anderson[30], A. Andreazza[89a,89b], V. Andrei[58a], M-L. Andrieux[55], X.S. Anduaga[70], A. Angerami[34], F. Anghinolfi[29], N. Anjos[124a], A. Annovi[47], A. Antonaki[8], M. Antonelli[47], S. Antonelli[19a,19b], A. Antonov[96], J. Antos[144b], F. Anulli[132a], S. Aoun[83], L. Aperio Bella[4], R. Apolle[118,c], G. Arabidze[88], I. Aracena[143], Y. Arai[66], A.T.H. Arce[44], J.P. Archambault[28], S. Arfaoui[29,d], J-F. Arguin[14], E. Arik[18a,*], M. Arik[18a], A.J. Armbruster[87], O. Arnaez[81], C. Arnault[115], A. Artamonov[95], G. Artoni[132a,132b], D. Arutinov[20], S. Asai[155], R. Asfandiyarov[172], S. Ask[27], B. Åsman[146a,146b], L. Asquith[5], K. Assamagan[24], A. Astbury[169], A. Astvatsatourov[52], G. Atoian[175], B. Aubert[4], B. Auerbach[175], E. Auge[115], K. Augsten[127], M. Aurousseau[145a], N. Austin[73], R. Avramidou[9], D. Axen[168], C. Ay[54], G. Azuelos[93,e], Y. Azuma[155], M.A. Baak[29], G. Baccaglioni[89a], C. Bacci[134a,134b], A.M. Bach[14], H. Bachacou[136], K. Bachas[29], G. Bachy[29], M. Backes[49], M. Backhaus[20], E. Badescu[25a], P. Bagnaia[132a,132b], S. Bahinipati[2], Y. Bai[32a], D.C. Bailey[158], T. Bain[158], J.T. Baines[129], O.K. Baker[175], M.D. Baker[24], S. Baker[77], F. Baltasar Dos Santos Pedrosa[29], E. Banas[38], P. Banerjee[93], Sw. Banerjee[169], D. Banfi[29], A. Bangert[137], V. Bansal[169], H.S. Bansil[17], L. Barak[171], S.P. Baranov[94], A. Barashkou[65], A. Barbaro Galtieri[14], T. Barber[27], E.L. Barberio[86], D. Barberis[50a,50b], M. Barbero[20], D.Y. Bardin[65], T. Barillari[99], M. Barisonzi[174], T. Barklow[143], N. Barlow[27], B.M. Barnett[129], R.M. Barnett[14], A. Baroncelli[134a], G. Barone[49], A.J. Barr[118], F. Barreiro[80], J. Barreiro Guimarães da Costa[57], P. Barrillon[115], R. Bartoldus[143], A.E. Barton[71], D. Bartsch[20], V. Bartsch[149], R.L. Bates[53], L. Batkova[144a], J.R. Batley[27], A. Battaglia[16], M. Battistin[29], G. Battistoni[89a], F. Bauer[136], H.S. Bawa[143,f], B. Beare[158], T. Beau[78], P.H. Beauchemin[118], R. Beccherle[50a], P. Bechtle[41], H.P. Beck[16], M. Beckingham[48], K.H. Becks[174], A.J. Beddall[18c], A. Beddall[18c], S. Bedikian[175], V.A. Bednyakov[65], C.P. Bee[83], M. Begel[24], S. Behar Harpaz[152], P.K. Behera[63], M. Beimforde[99], C. Belanger-Champagne[166], P.J. Bell[49], W.H. Bell[49], G. Bella[153], L. Bellagamba[19a], F. Bellina[29], M. Bellomo[119a], A. Belloni[57], O. Beloborodova[107], K. Belotskiy[96], O. Beltramello[29], S. Ben Ami[152], O. Benary[153], D. Benchekroun[135a], C. Benchouk[83], M. Bendel[81], B.H. Benedict[163], N. Benekos[165], Y. Benhammou[153],

D.P. Benjamin[44], M. Benoit[115], J.R. Bensinger[22], K. Benslama[130], S. Bentvelsen[105], D. Berge[29], E. Bergeaas Kuutmann[41], N. Berger[4], F. Berghaus[169], E. Berglund[49], J. Beringer[14], K. Bernardet[83], P. Bernat[77], R. Bernhard[48], C. Bernius[24], T. Berry[76], A. Bertin[19a,19b], F. Bertinelli[29], F. Bertolucci[122a,122b], M.I. Besana[89a,89b], N. Besson[136], S. Bethke[99], W. Bhimji[45], R.M. Bianchi[29], M. Bianco[72a,72b], O. Biebel[98], S.P. Bieniek[77], J. Biesiada[14], M. Biglietti[134a,134b], H. Bilokon[47], M. Bindi[19a,19b], S. Binet[115], A. Bingul[18c], C. Bini[132a,132b], C. Biscarat[177], U. Bitenc[48], K.M. Black[21], R.E. Blair[5], J.-B. Blanchard[115], G. Blanchot[29], T. Blazek[144a], C. Blocker[22], J. Blocki[38], A. Blondel[49], W. Blum[81], U. Blumenschein[54], G.J. Bobbink[105], V.B. Bobrovnikov[107], S.S. Bocchetta[79], A. Bocci[44], C.R. Boddy[118], M. Boehler[41], J. Boek[174], N. Boelaert[35], S. Böser[77], J.A. Bogaerts[29], A. Bogdanchikov[107], A. Bogouch[90,*], C. Bohm[146a], V. Boisvert[76], T. Bold[163,g], V. Boldea[25a], N.M. Bolnet[136], M. Bona[75], V.G. Bondarenko[96], M. Boonekamp[136], G. Boorman[76], C.N. Booth[139], S. Bordoni[78], C. Borer[16], A. Borisov[128], G. Borissov[71], I. Borjanovic[12a], S. Borroni[132a,132b], K. Bos[105], D. Boscherini[19a], M. Bosman[11], H. Boterenbrood[105], D. Botterill[129], J. Bouchami[93], J. Boudreau[123], E.V. Bouhova-Thacker[71], C. Boulahouache[123], C. Bourdarios[115], N. Bousson[83], A. Boveia[30], J. Boyd[29], I.R. Boyko[65], N.I. Bozhko[128], I. Bozovic-Jelisavcic[12b], J. Bracinik[17], A. Braem[29], P. Branchini[134a], G.W. Brandenburg[57], A. Brandt[7], G. Brandt[15], O. Brandt[54], U. Bratzler[156], B. Brau[84], J.E. Brau[114], H.M. Braun[174], B. Brelier[158], J. Bremer[29], R. Brenner[166], S. Bressler[152], D. Breton[115], D. Britton[53], F.M. Brochu[27], I. Brock[20], R. Brock[88], T.J. Brodbeck[71], E. Brodet[153], F. Broggi[89a], C. Bromberg[88], G. Brooijmans[34], W.K. Brooks[31b], G. Brown[82], H. Brown[7], E. Brubaker[30], P.A. Bruckman de Renstrom[38], D. Bruncko[144b], R. Bruneliere[48], S. Brunet[61], A. Bruni[19a], G. Bruni[19a], M. Bruschi[19a], T. Buanes[13], F. Bucci[49], J. Buchanan[118], N.J. Buchanan[2], P. Buchholz[141], R.M. Buckingham[118], A.G. Buckley[45], S.I. Buda[25a], I.A. Budagov[65], B. Budick[108], V. Büscher[81], L. Bugge[117], D. Buira-Clark[118], O. Bulekov[96], M. Bunse[42], T. Buran[117], H. Burckhart[29], S. Burdin[73], T. Burgess[13], S. Burke[129], E. Busato[33], P. Bussey[53], C.P. Buszello[166], F. Butin[29], B. Butler[143], J.M. Butler[21], C.M. Buttar[53], J.M. Butterworth[77], W. Buttinger[27], T. Byatt[77], S. Cabrera Urbán[167], D. Caforio[19a,19b], O. Cakir[3a], P. Calafiura[14], G. Calderini[78], P. Calfayan[98], R. Calkins[106], L.P. Caloba[23a], R. Caloi[132a,132b], D. Calvet[33], S. Calvet[33], R. Camacho Toro[33], A. Camard[78], P. Camarri[133a,133b], M. Cambiaghi[119a,119b], D. Cameron[117], J. Cammin[20], S. Campana[29], M. Campanelli[77], V. Canale[102a,102b], F. Canelli[30], A. Canepa[159a], J. Cantero[80], L. Capasso[102a,102b], M.D.M. Capeans Garrido[29], I. Caprini[25a], M. Caprini[25a], D. Capriotti[99], M. Capua[36a,36b], R. Caputo[148], C. Caramarcu[25a], R. Cardarelli[133a], T. Carli[29], G. Carlino[102a], L. Carminati[89a,89b], B. Caron[159a], S. Caron[48], G.D. Carrillo Montoya[172], A.A. Carter[75], J.R. Carter[27], J. Carvalho[124a,h], D. Casadei[108], M.P. Casado[11], M. Cascella[122a,122b], C. Caso[50a,50b,*], A.M. Castaneda Hernandez[172], E. Castaneda-Miranda[172], V. Castillo Gimenez[167], N.F. Castro[124a], G. Cataldi[72a], F. Cataneo[29], A. Catinaccio[29], J.R. Catmore[71], A. Cattai[29], G. Cattani[133a,133b], S. Caughron[88], D. Cauz[164a,164c], P. Cavalleri[78], D. Cavalli[89a], M. Cavalli-Sforza[11], V. Cavasinni[122a,122b], A. Cazzato[72a,72b], F. Ceradini[134a,134b], A.S. Cerqueira[23a], A. Cerri[29], L. Cerrito[75], F. Cerutti[47],

S.A. Cetin[18b], F. Cevenini[102a,102b], A. Chafaq[135a], D. Chakraborty[106], K. Chan[2], B. Chapleau[85], J.D. Chapman[27], J.W. Chapman[87], E. Chareyre[78], D.G. Charlton[17], V. Chavda[82], S. Cheatham[85], S. Chekanov[5], S.V. Chekulaev[159a], G.A. Chelkov[65], M.A. Chelstowska[104], C. Chen[64], H. Chen[24], L. Chen[2], S. Chen[32c], T. Chen[32c], X. Chen[172], S. Cheng[32a], A. Cheplakov[65], V.F. Chepurnov[65], R. Cherkaoui El Moursli[135e], V. Chernyatin[24], E. Cheu[6], S.L. Cheung[158], L. Chevalier[136], G. Chiefari[102a,102b], L. Chikovani[51], J.T. Childers[58a], A. Chilingarov[71], G. Chiodini[72a], M.V. Chizhov[65], G. Choudalakis[30], S. Chouridou[137], I.A. Christidi[77], A. Christov[48], D. Chromek-Burckhart[29], M.L. Chu[151], J. Chudoba[125], G. Ciapetti[132a,132b], K. Ciba[37], A.K. Ciftci[3a], R. Ciftci[3a], D. Cinca[33], V. Cindro[74], M.D. Ciobotaru[163], C. Ciocca[19a,19b], A. Ciocio[14], M. Cirilli[87], M. Ciubancan[25a], A. Clark[49], P.J. Clark[45], W. Cleland[123], J.C. Clemens[83], B. Clement[55], C. Clement[146a,146b], R.W. Clifft[129], Y. Coadou[83], M. Cobal[164a,164c], A. Coccaro[50a,50b], J. Cochran[64], P. Coe[118], J.G. Cogan[143], J. Coggeshall[165], E. Cogneras[177], C.D. Cojocaru[28], J. Colas[4], A.P. Colijn[105], C. Collard[115], N.J. Collins[17], C. Collins-Tooth[53], J. Collot[55], G. Colon[84], P. Conde Muiño[124a], E. Coniavitis[118], M.C. Conidi[11], M. Consonni[104], V. Consorti[48], S. Constantinescu[25a], C. Conta[119a,119b], F. Conventi[102a,i], J. Cook[29], M. Cooke[14], B.D. Cooper[77], A.M. Cooper-Sarkar[118], N.J. Cooper-Smith[76], K. Copic[34], T. Cornelissen[50a,50b], M. Corradi[19a], F. Corriveau[85,j], A. Cortes-Gonzalez[165], G. Cortiana[99], G. Costa[89a], M.J. Costa[167], D. Costanzo[139], T. Costin[30], D. Côté[29], R. Coura Torres[23a], L. Courneyea[169], G. Cowan[76], C. Cowden[27], B.E. Cox[82], K. Cranmer[108], F. Crescioli[122a,122b], M. Cristinziani[20], G. Crosetti[36a,36b], R. Crupi[72a,72b], S. Crépé-Renaudin[55], C.-M. Cuciuc[25a], C. Cuenca Almenar[175], T. Cuhadar Donszelmann[139], S. Cuneo[50a,50b], M. Curatolo[47], C.J. Curtis[17], P. Cwetanski[61], H. Czirr[141], Z. Czyczula[117], S. D'Auria[53], M. D'Onofrio[73], A. D'Orazio[132a,132b], A. Da Rocha Gesualdi Mello[23a], P.V.M. Da Silva[23a], C. Da Via[82], W. Dabrowski[37], A. Dahlhoff[48], T. Dai[87], C. Dallapiccola[84], M. Dam[35], M. Dameri[50a,50b], D.S. Damiani[137], H.O. Danielsson[29], D. Dannheim[99], V. Dao[49], G. Darbo[50a], G.L. Darlea[25b], C. Daum[105], J.P. Dauvergne [29], W. Davey[86], T. Davidek[126], N. Davidson[86], R. Davidson[71], E. Davies[118,c], M. Davies[93], A.R. Davison[77], Y. Davygora[58a], E. Dawe[142], I. Dawson[139], J.W. Dawson[5,*], R.K. Daya[39], K. De[7], R. de Asmundis[102a], S. De Castro[19a,19b], P.E. De Castro Faria Salgado[24], S. De Cecco[78], J. de Graat[98], N. De Groot[104], P. de Jong[105], C. De La Taille[115], H. De la Torre[80], B. De Lotto[164a,164c], L. De Mora[71], L. De Nooij[105], M. De Oliveira Branco[29], D. De Pedis[132a], P. de Saintignon[55], A. De Salvo[132a], U. De Sanctis[164a,164c], A. De Santo[149], J.B. De Vivie De Regie[115], S. Dean[77], D.V. Dedovich[65], J. Degenhardt[120], M. Dehchar[118], M. Deile[98], C. Del Papa[164a,164c], J. Del Peso[80], T. Del Prete[122a,122b], A. Dell'Acqua[29], L. Dell'Asta[89a,89b], M. Della Pietra[102a,i], D. della Volpe[102a,102b], M. Delmastro[29], P. Delpierre[83], N. Delruelle[29], P.A. Delsart[55], C. Deluca[148], S. Demers[175], M. Demichev[65], B. Demirkoz[11,k], J. Deng[163], S.P. Denisov[128], D. Derendarz[38], J.E. Derkaoui[135d], F. Derue[78], P. Dervan[73], K. Desch[20], E. Devetak[148], P.O. Deviveiros[158], A. Dewhurst[129], B. DeWilde[148], S. Dhaliwal[158], R. Dhullipudi[24,l], A. Di Ciaccio[133a,133b], L. Di Ciaccio[4], A. Di Girolamo[29], B. Di Girolamo[29],

S. Di Luise[134a,134b], A. Di Mattia[88], B. Di Micco[29], R. Di Nardo[133a,133b], A. Di Simone[133a,133b], R. Di Sipio[19a,19b], M.A. Diaz[31a], F. Diblen[18c], E.B. Diehl[87], H. Dietl[99], J. Dietrich[41], T.A. Dietzsch[58a], S. Diglio[115], K. Dindar Yagci[39], J. Dingfelder[20], C. Dionisi[132a,132b], P. Dita[25a], S. Dita[25a], F. Dittus[29], F. Djama[83], R. Djilkibaev[108], T. Djobava[51], M.A.B. do Vale[23a], A. Do Valle Wemans[124a], T.K.O. Doan[4], M. Dobbs[85], R. Dobinson [29,*], D. Dobos[42], E. Dobson[29], M. Dobson[163], J. Dodd[34], O.B. Dogan[18a,*], C. Doglioni[118], T. Doherty[53], Y. Doi[66,*], J. Dolejsi[126], I. Dolenc[74], Z. Dolezal[126], B.A. Dolgoshein[96,*], T. Dohmae[155], M. Donadelli[23b], M. Donega[120], J. Donini[55], J. Dopke[29], A. Doria[102a], A. Dos Anjos[172], M. Dosil[11], A. Dotti[122a,122b], M.T. Dova[70], J.D. Dowell[17], A.D. Doxiadis[105], A.T. Doyle[53], Z. Drasal[126], J. Drees[174], N. Dressnandt[120], H. Drevermann[29], C. Driouichi[35], M. Dris[9], J. Dubbert[99], T. Dubbs[137], S. Dube[14], E. Duchovni[171], G. Duckeck[98], A. Dudarev[29], F. Dudziak[64], M. Dührssen [29], I.P. Duerdoth[82], L. Duflot[115], M-A. Dufour[85], M. Dunford[29], H. Duran Yildiz[3b], R. Duxfield[139], M. Dwuznik[37], F. Dydak [29], D. Dzahini[55], M. Düren[52], W.L. Ebenstein[44], J. Ebke[98], S. Eckert[48], S. Eckweiler[81], K. Edmonds[81], C.A. Edwards[76], N.C. Edwards[53], W. Ehrenfeld[41], T. Ehrich[99], T. Eifert[29], G. Eigen[13], K. Einsweiler[14], E. Eisenhandler[75], T. Ekelof[166], M. El Kacimi[135c], M. Ellert[166], S. Elles[4], F. Ellinghaus[81], K. Ellis[75], N. Ellis[29], J. Elmsheuser[98], M. Elsing[29], R. Ely[14], D. Emeliyanov[129], R. Engelmann[148], A. Engl[98], B. Epp[62], A. Eppig[87], J. Erdmann[54], A. Ereditato[16], D. Eriksson[146a], J. Ernst[1], M. Ernst[24], J. Ernwein[136], D. Errede[165], S. Errede[165], E. Ertel[81], M. Escalier[115], C. Escobar[167], X. Espinal Curull[11], B. Esposito[47], F. Etienne[83], A.I. Etienvre[136], E. Etzion[153], D. Evangelakou[54], H. Evans[61], L. Fabbri[19a,19b], C. Fabre[29], R.M. Fakhrutdinov[128], S. Falciano[132a], A.C. Falou[115], Y. Fang[172], M. Fanti[89a,89b], A. Farbin[7], A. Farilla[134a], J. Farley[148], T. Farooque[158], S.M. Farrington[118], P. Farthouat[29], P. Fassnacht[29], D. Fassouliotis[8], B. Fatholahzadeh[158], A. Favareto[89a,89b], L. Fayard[115], S. Fazio[36a,36b], R. Febbraro[33], P. Federic[144a], O.L. Fedin[121], I. Fedorko[29], W. Fedorko[88], M. Fehling-Kaschek[48], L. Feligioni[83], D. Fellmann[5], C.U. Felzmann[86], C. Feng[32d], E.J. Feng[30], A.B. Fenyuk[128], J. Ferencei[144b], J. Ferland[93], W. Fernando[109], S. Ferrag[53], J. Ferrando[53], V. Ferrara[41], A. Ferrari[166], P. Ferrari[105], R. Ferrari[119a], A. Ferrer[167], M.L. Ferrer[47], D. Ferrere[49], C. Ferretti[87], A. Ferretto Parodi[50a,50b], M. Fiascaris[30], F. Fiedler[81], A. Filipčič[74], A. Filippas[9], F. Filthaut[104], M. Fincke-Keeler[169], M.C.N. Fiolhais[124a,h], L. Fiorini[167], A. Firan[39], G. Fischer[41], P. Fischer [20], M.J. Fisher[109], S.M. Fisher[129], M. Flechl[48], I. Fleck[141], J. Fleckner[81], P. Fleischmann[173], S. Fleischmann[174], T. Flick[174], L.R. Flores Castillo[172], M.J. Flowerdew[99], F. Föhlisch[58a], M. Fokitis[9], T. Fonseca Martin[16], D.A. Forbush[138], A. Formica[136], A. Forti[82], D. Fortin[159a], J.M. Foster[82], D. Fournier[115], A. Foussat[29], A.J. Fowler[44], K. Fowler[137], H. Fox[71], P. Francavilla[122a,122b], S. Franchino[119a,119b], D. Francis[29], T. Frank[171], M. Franklin[57], S. Franz[29], M. Fraternali[119a,119b], S. Fratina[120], S.T. French[27], R. Froeschl[29], D. Froidevaux[29], J.A. Frost[27], C. Fukunaga[156], E. Fullana Torregrosa[29], J. Fuster[167], C. Gabaldon[29], O. Gabizon[171], T. Gadfort[24], S. Gadomski[49], G. Gagliardi[50a,50b], P. Gagnon[61], C. Galea[98], E.J. Gallas[118], M.V. Gallas[29], V. Gallo[16], B.J. Gallop[129], P. Gallus[125], E. Galyaev[40], K.K. Gan[109],

Y.S. Gao[143,f], V.A. Gapienko[128], A. Gaponenko[14], F. Garberson[175], M. Garcia-Sciveres[14], C. García[167], J.E. García Navarro[49], R.W. Gardner[30], N. Garelli[29], H. Garitaonandia[105], V. Garonne[29], J. Garvey[17], C. Gatti[47], G. Gaudio[119a], O. Gaumer[49], B. Gaur[141], L. Gauthier[136], I.L. Gavrilenko[94], C. Gay[168], G. Gaycken[20], J-C. Gayde[29], E.N. Gazis[9], P. Ge[32d], C.N.P. Gee[129], D.A.A. Geerts[105], Ch. Geich-Gimbel[20], K. Gellerstedt[146a,146b], C. Gemme[50a], A. Gemmell[53], M.H. Genest[98], S. Gentile[132a,132b], M. George[54], S. George[76], P. Gerlach[174], A. Gershon[153], C. Geweniger[58a], H. Ghazlane[135b], P. Ghez[4], N. Ghodbane[33], B. Giacobbe[19a], S. Giagu[132a,132b], V. Giakoumopoulou[8], V. Giangiobbe[122a,122b], F. Gianotti[29], B. Gibbard[24], A. Gibson[158], S.M. Gibson[29], L.M. Gilbert[118], M. Gilchriese[14], V. Gilewsky[91], D. Gillberg[28], A.R. Gillman[129], D.M. Gingrich[2,e], J. Ginzburg[153], N. Giokaris[8], R. Giordano[102a,102b], F.M. Giorgi[15], P. Giovannini[99], P.F. Giraud[136], D. Giugni[89a], M. Giunta[132a,132b], P. Giusti[19a], B.K. Gjelsten[117], L.K. Gladilin[97], C. Glasman[80], J. Glatzer[48], A. Glazov[41], K.W. Glitza[174], G.L. Glonti[65], J. Godfrey[142], J. Godlewski[29], M. Goebel[41], T. Göpfert[43], C. Goeringer[81], C. Gössling[42], T. Göttfert[99], S. Goldfarb[87], D. Goldin[39], T. Golling[175], S.N. Golovnia[128], A. Gomes[124a,b], L.S. Gomez Fajardo[41], R. Gonçalo[76], J. Goncalves Pinto Firmino Da Costa[41], L. Gonella[20], A. Gonidec[29], S. Gonzalez[172], S. González de la Hoz[167], M.L. Gonzalez Silva[26], S. Gonzalez-Sevilla[49], J.J. Goodson[148], L. Goossens[29], P.A. Gorbounov[95], H.A. Gordon[24], I. Gorelov[103], G. Gorfine[174], B. Gorini[29], E. Gorini[72a,72b], A. Gorišek[74], E. Gornicki[38], S.A. Gorokhov[128], V.N. Goryachev[128], B. Gosdzik[41], A.T. Goshaw[5], M. Gosselink[105], M.I. Gostkin[65], M. Gouanère[4], I. Gough Eschrich[163], M. Gouighri[135a], D. Goujdami[135c], M.P. Goulette[49], A.G. Goussiou[138], C. Goy[4], I. Grabowska-Bold[163,g], V. Grabski[176], P. Grafström[29], C. Grah[174], K-J. Grahn[41], F. Grancagnolo[72a], S. Grancagnolo[15], V. Grassi[148], V. Gratchev[121], N. Grau[34], H.M. Gray[29], J.A. Gray[148], E. Graziani[134a], O.G. Grebenyuk[121], D. Greenfield[129], T. Greenshaw[73], Z.D. Greenwood[24,l], I.M. Gregor[41], P. Grenier[143], E. Griesmayer[46], J. Griffiths[138], N. Grigalashvili[65], A.A. Grillo[137], S. Grinstein[11], Ph. Gris[33], Y.V. Grishkevich[97], J.-F. Grivaz[115], J. Grognuz[29], M. Groh[99], E. Gross[171], J. Grosse-Knetter[54], J. Groth-Jensen[171], K. Grybel[141], V.J. Guarino[5], D. Guest[175], C. Guicheney[33], A. Guida[72a,72b], T. Guillemin[4], S. Guindon[54], H. Guler[85,m], J. Gunther[125], B. Guo[158], J. Guo[34], A. Gupta[30], Y. Gusakov[65], V.N. Gushchin[128], A. Gutierrez[93], P. Gutierrez[111], N. Guttman[153], O. Gutzwiller[172], C. Guyot[136], C. Gwenlan[118], C.B. Gwilliam[73], A. Haas[143], S. Haas[29], C. Haber[14], R. Hackenburg[24], H.K. Hadavand[39], D.R. Hadley[17], P. Haefner[99], F. Hahn[29], S. Haider[29], Z. Hajduk[38], H. Hakobyan[176], J. Haller[54], K. Hamacher[174], P. Hamal[113], A. Hamilton[49], S. Hamilton[161], H. Han[32a], L. Han[32b], K. Hanagaki[116], M. Hance[120], C. Handel[81], P. Hanke[58a], J.R. Hansen[35], J.B. Hansen[35], J.D. Hansen[35], P.H. Hansen[35], P. Hansson[143], K. Hara[160], G.A. Hare[137], T. Harenberg[174], S. Harkusha[90], D. Harper[87], R.D. Harrington[21], O.M. Harris[138], K. Harrison[17], J. Hartert[48], F. Hartjes[105], T. Haruyama[66], A. Harvey[56], S. Hasegawa[101], Y. Hasegawa[140], S. Hassani[136], M. Hatch[29], D. Hauff[99], S. Haug[16], M. Hauschild[29], R. Hauser[88], M. Havranek[20], B.M. Hawes[118], C.M. Hawkes[17], R.J. Hawkings[29], D. Hawkins[163], T. Hayakawa[67], D Hayden[76], H.S. Hayward[73], S.J. Haywood[129], E. Hazen[21], M. He[32d],

S.J. Head[17], V. Hedberg[79], L. Heelan[7], S. Heim[88], B. Heinemann[14], S. Heisterkamp[35], L. Helary[4], M. Heldmann[48], M. Heller[115], S. Hellman[146a,146b], C. Helsens[11], R.C.W. Henderson[71], M. Henke[58a], A. Henrichs[54], A.M. Henriques Correia[29], S. Henrot-Versille[115], F. Henry-Couannier[83], C. Hensel[54], T. Henß[174], C.M. Hernandez[7], Y. Hernández Jiménez[167], R. Herrberg[15], A.D. Hershenhorn[152], G. Herten[48], R. Hertenberger[98], L. Hervas[29], N.P. Hessey[105], A. Hidvegi[146a], E. Higón-Rodriguez[167], D. Hill[5,*], J.C. Hill[27], N. Hill[5], K.H. Hiller[41], S. Hillert[20], S.J. Hillier[17], I. Hinchliffe[14], E. Hines[120], M. Hirose[116], F. Hirsch[42], D. Hirschbuehl[174], J. Hobbs[148], N. Hod[153], M.C. Hodgkinson[139], P. Hodgson[139], A. Hoecker[29], M.R. Hoeferkamp[103], J. Hoffman[39], D. Hoffmann[83], M. Hohlfeld[81], M. Holder[141], A. Holmes[118], S.O. Holmgren[146a], T. Holy[127], J.L. Holzbauer[88], Y. Homma[67], T.M. Hong[120], L. Hooft van Huysduynen[108], T. Horazdovsky[127], C. Horn[143], S. Horner[48], K. Horton[118], J-Y. Hostachy[55], S. Hou[151], M.A. Houlden[73], A. Hoummada[135a], J. Howarth[82], D.F. Howell[118], I. Hristova [41], J. Hrivnac[115], I. Hruska[125], T. Hryn'ova[4], P.J. Hsu[175], S.-C. Hsu[14], G.S. Huang[111], Z. Hubacek[127], F. Hubaut[83], F. Huegging[20], T.B. Huffman[118], E.W. Hughes[34], G. Hughes[71], R.E. Hughes-Jones[82], M. Huhtinen[29], P. Hurst[57], M. Hurwitz[14], U. Husemann[41], N. Huseynov[65,n], J. Huston[88], J. Huth[57], G. Iacobucci[49], G. Iakovidis[9], M. Ibbotson[82], I. Ibragimov[141], R. Ichimiya[67], L. Iconomidou-Fayard[115], J. Idarraga[115], M. Idzik[37], P. Iengo[102a,102b], O. Igonkina[105], Y. Ikegami[66], M. Ikeno[66], Y. Ilchenko[39], D. Iliadis[154], D. Imbault[78], M. Imhaeuser[174], M. Imori[155], T. Ince[20], J. Inigo-Golfin[29], P. Ioannou[8], M. Iodice[134a], G. Ionescu[4], A. Irles Quiles[167], K. Ishii[66], A. Ishikawa[67], M. Ishino[66], R. Ishmukhametov[39], C. Issever[118], S. Istin[18a], Y. Itoh[101], A.V. Ivashin[128], W. Iwanski[38], H. Iwasaki[66], J.M. Izen[40], V. Izzo[102a], B. Jackson[120], J.N. Jackson[73], P. Jackson[143], M.R. Jaekel[29], V. Jain[61], K. Jakobs[48], S. Jakobsen[35], J. Jakubek[127], D.K. Jana[111], E. Jankowski[158], E. Jansen[77], A. Jantsch[99], M. Janus[20], G. Jarlskog[79], L. Jeanty[57], K. Jelen[37], I. Jen-La Plante[30], P. Jenni[29], A. Jeremie[4], P. Jež[35], S. Jézéquel[4], M.K. Jha[19a], H. Ji[172], W. Ji[81], J. Jia[148], Y. Jiang[32b], M. Jimenez Belenguer[41], G. Jin[32b], S. Jin[32a], O. Jinnouchi[157], M.D. Joergensen[35], D. Joffe[39], L.G. Johansen[13], M. Johansen[146a,146b], K.E. Johansson[146a], P. Johansson[139], S. Johnert[41], K.A. Johns[6], K. Jon-And[146a,146b], G. Jones[82], R.W.L. Jones[71], T.W. Jones[77], T.J. Jones[73], O. Jonsson[29], C. Joram[29], P.M. Jorge[124a,b], J. Joseph[14], X. Ju[130], V. Juranek[125], P. Jussel[62], V.V. Kabachenko[128], S. Kabana[16], M. Kaci[167], A. Kaczmarska[38], P. Kadlecik[35], M. Kado[115], H. Kagan[109], M. Kagan[57], S. Kaiser[99], E. Kajomovitz[152], S. Kalinin[174], L.V. Kalinovskaya[65], S. Kama[39], N. Kanaya[155], M. Kaneda[29], T. Kanno[157], V.A. Kantserov[96], J. Kanzaki[66], B. Kaplan[175], A. Kapliy[30], J. Kaplon[29], D. Kar[43], M. Karagoz[118], M. Karnevskiy[41], K. Karr[5], V. Kartvelishvili[71], A.N. Karyukhin[128], L. Kashif[172], A. Kasmi[39], R.D. Kass[109], A. Kastanas[13], M. Kataoka[4], Y. Kataoka[155], E. Katsoufis[9], J. Katzy[41], V. Kaushik[6], K. Kawagoe[67], T. Kawamoto[155], G. Kawamura[81], M.S. Kayl[105], V.A. Kazanin[107], M.Y. Kazarinov[65], J.R. Keates[82], R. Keeler[169], R. Kehoe[39], M. Keil[54], G.D. Kekelidze[65], M. Kelly[82], J. Kennedy[98], C.J. Kenney[143], M. Kenyon[53], O. Kepka[125], N. Kerschen[29], B.P. Kerševan[74], S. Kersten[174], K. Kessoku[155], C. Ketterer[48], J. Keung[158], M. Khakzad[28], F. Khalil-zada[10], H. Khandanyan[165], A. Khanov[112], D. Kharchenko[65], A. Khodinov[96], A.G. Kholodenko[128], A. Khomich[58a],

T.J. Khoo[27], G. Khoriauli[20], A. Khoroshilov[174], N. Khovanskiy[65], V. Khovanskiy[95], E. Khramov[65], J. Khubua[51], H. Kim[7], M.S. Kim[2], P.C. Kim[143], S.H. Kim[160], N. Kimura[170], O. Kind[15], B.T. King[73], M. King[67], R.S.B. King[118], J. Kirk[129], G.P. Kirsch[118], L.E. Kirsch[22], A.E. Kiryunin[99], D. Kisielewska[37], T. Kittelmann[123], A.M. Kiver[128], H. Kiyamura[67], E. Kladiva[144b], J. Klaiber-Lodewigs[42], M. Klein[73], U. Klein[73], K. Kleinknecht[81], M. Klemetti[85], A. Klier[171], A. Klimentov[24], R. Klingenberg[42], E.B. Klinkby[35], T. Klioutchnikova[29], P.F. Klok[104], S. Klous[105], E.-E. Kluge[58a], T. Kluge[73], P. Kluit[105], S. Kluth[99], E. Kneringer[62], J. Knobloch[29], E.B.F.G. Knoops[83], A. Knue[54], B.R. Ko[44], T. Kobayashi[155], M. Kobel[43], M. Kocian[143], A. Kocnar[113], P. Kodys[126], K. Köneke[29], A.C. König[104], S. Koenig[81], L. Köpke[81], F. Koetsveld[104], P. Koevesarki[20], T. Koffas[29], E. Koffeman[105], F. Kohn[54], Z. Kohout[127], T. Kohriki[66], T. Koi[143], T. Kokott[20], G.M. Kolachev[107], H. Kolanoski[15], V. Kolesnikov[65], I. Koletsou[89a], J. Koll[88], D. Kollar[29], M. Kollefrath[48], S.D. Kolya[82], A.A. Komar[94], J.R. Komaragiri[142], Y. Komori[155], T. Kondo[66], T. Kono[41,o], A.I. Kononov[48], R. Konoplich[108,p], N. Konstantinidis[77], A. Kootz[174], S. Koperny[37], S.V. Kopikov[128], K. Korcyl[38], K. Kordas[154], V. Koreshev[128], A. Korn[14], A. Korol[107], I. Korolkov[11], E.V. Korolkova[139], V.A. Korotkov[128], O. Kortner[99], S. Kortner[99], V.V. Kostyukhin[20], M.J. Kotamäki[29], S. Kotov[99], V.M. Kotov[65], A. Kotwal[44], C. Kourkoumelis[8], V. Kouskoura[154], A. Koutsman[105], R. Kowalewski[169], T.Z. Kowalski[37], W. Kozanecki[136], A.S. Kozhin[128], V. Kral[127], V.A. Kramarenko[97], G. Kramberger[74], O. Krasel[42], M.W. Krasny[78], A. Krasznahorkay[108], J. Kraus[88], A. Kreisel[153], F. Krejci[127], J. Kretzschmar[73], N. Krieger[54], P. Krieger[158], K. Kroeninger[54], H. Kroha[99], J. Kroll[120], J. Kroseberg[20], J. Krstic[12a], U. Kruchonak[65], H. Krüger[20], T. Kruker[16], Z.V. Krumshteyn[65], A. Kruth[20], T. Kubota[86], S. Kuehn[48], A. Kugel[58c], T. Kuhl[174], D. Kuhn[62], V. Kukhtin[65], Y. Kulchitsky[90], S. Kuleshov[31b], C. Kummer[98], M. Kuna[78], N. Kundu[118], J. Kunkle[120], A. Kupco[125], H. Kurashige[67], M. Kurata[160], Y.A. Kurochkin[90], V. Kus[125], W. Kuykendall[138], M. Kuze[157], P. Kuzhir[91], O. Kvasnicka[125], J. Kvita[29], R. Kwee[15], A. La Rosa[172], L. La Rotonda[36a,36b], L. Labarga[80], J. Labbe[4], S. Lablak[135a], C. Lacasta[167], F. Lacava[132a,132b], H. Lacker[15], D. Lacour[78], V.R. Lacuesta[167], E. Ladygin[65], R. Lafaye[4], B. Laforge[78], T. Lagouri[80], S. Lai[48], E. Laisne[55], M. Lamanna[29], C.L. Lampen[6], W. Lampl[6], E. Lancon[136], U. Landgraf[48], M.P.J. Landon[75], H. Landsman[152], J.L. Lane[82], C. Lange[41], A.J. Lankford[163], F. Lanni[24], K. Lantzsch[29], V.V. Lapin[128,*], S. Laplace[78], C. Lapoire[20], J.F. Laporte[136], T. Lari[89a], A.V. Larionov [128], A. Larner[118], C. Lasseur[29], M. Lassnig[29], W. Lau[118], P. Laurelli[47], A. Lavorato[118], W. Lavrijsen[14], P. Laycock[73], A.B. Lazarev[65], A. Lazzaro[89a,89b], O. Le Dortz[78], E. Le Guirriec[83], C. Le Maner[158], E. Le Menedeu[136], A. Lebedev[64], C. Lebel[93], T. LeCompte[5], F. Ledroit-Guillon[55], H. Lee[105], J.S.H. Lee[150], S.C. Lee[151], L. Lee[175], M. Lefebvre[169], M. Legendre[136], A. Leger[49], B.C. LeGeyt[120], F. Legger[98], C. Leggett[14], M. Lehmacher[20], G. Lehmann Miotto[29], X. Lei[6], M.A.L. Leite[23b], R. Leitner[126], D. Lellouch[171], J. Lellouch[78], M. Leltchouk[34], V. Lendermann[58a], K.J.C. Leney[145b], T. Lenz[174], G. Lenzen[174], B. Lenzi[29], K. Leonhardt[43], S. Leontsinis[9], C. Leroy[93], J-R. Lessard[169], J. Lesser[146a], C.G. Lester[27], A. Leung Fook Cheong[172], J. Levêque[4], D. Levin[87], L.J. Levinson[171], M.S. Levitski[128],

M. Lewandowska[21], A. Lewis[118], G.H. Lewis[108], A.M. Leyko[20], M. Leyton[15], B. Li[83], H. Li[172], S. Li[32b,d], X. Li[87], Z. Liang[39], Z. Liang[118,q], B. Liberti[133a], P. Lichard[29], M. Lichtnecker[98], K. Lie[165], W. Liebig[13], R. Lifshitz[152], J.N. Lilley[17], C. Limbach[20], A. Limosani[86], M. Limper[63], S.C. Lin[151,r], F. Linde[105], J.T. Linnemann[88], E. Lipeles[120], L. Lipinsky[125], A. Lipniacka[13], T.M. Liss[165], D. Lissauer[24], A. Lister[49], A.M. Litke[137], C. Liu[28], D. Liu[151,s], H. Liu[87], J.B. Liu[87], M Liu[44], M. Liu[32b], S. Liu[2], Y. Liu[32b], M. Livan[119a,119b], S.S.A. Livermore[118], A. Lleres[55], J. Llorente Merino[80], S.L. Lloyd[75], E. Lobodzinska[41], P. Loch[6], W.S. Lockman[137], S. Lockwitz[175], T. Loddenkoetter[20], F.K. Loebinger[82], A. Loginov[175], C.W. Loh[168], T. Lohse[15], K. Lohwasser[48], M. Lokajicek[125], J. Loken [118], V.P. Lombardo[4], R.E. Long[71], L. Lopes[124a,b], D. Lopez Mateos[34,t], M. Losada[162], P. Loscutoff[14], F. Lo Sterzo[132a,132b], M.J. Losty[159a], X. Lou[40], A. Lounis[115], K.F. Loureiro[162], J. Love[21], P.A. Love[71], A.J. Lowe[143,f], F. Lu[32a], L. Lu[39], H.J. Lubatti[138], C. Luci[132a,132b], A. Lucotte[55], A. Ludwig[43], D. Ludwig[41], I. Ludwig[48], J. Ludwig[48], F. Luehring[61], G. Luijckx[105], D. Lumb[48], L. Luminari[132a], E. Lund[117], B. Lund-Jensen[147], B. Lundberg[79], J. Lundberg[146a,146b], J. Lundquist[35], M. Lungwitz[81], A. Lupi[122a,122b], G. Lutz[99], D. Lynn[24], J. Lys[14], E. Lytken[79], H. Ma[24], L.L. Ma[172], J.A. Macana Goia[93], G. Maccarrone[47], A. Macchiolo[99], B. Maček[74], J. Machado Miguens[124a], D. Macina[49], R. Mackeprang[35], R.J. Madaras[14], W.F. Mader[43], R. Maenner[58c], T. Maeno[24], P. Mättig[174], S. Mättig[41], P.J. Magalhaes Martins[124a,h], L. Magnoni[29], E. Magradze[54], Y. Mahalalel[153], K. Mahboubi[48], G. Mahout[17], C. Maiani[132a,132b], C. Maidantchik[23a], A. Maio[124a,b], S. Majewski[24], Y. Makida[66], N. Makovec[115], P. Mal[6], Pa. Malecki[38], P. Malecki[38], V.P. Maleev[121], F. Malek[55], U. Mallik[63], D. Malon[5], S. Maltezos[9], V. Malyshev[107], S. Malyukov[29], R. Mameghani[98], J. Mamuzic[12b], A. Manabe[66], L. Mandelli[89a], I. Mandić[74], R. Mandrysch[15], J. Maneira[124a], P.S. Mangeard[88], I.D. Manjavidze[65], A. Mann[54], P.M. Manning[137], A. Manousakis-Katsikakis[8], B. Mansoulie[136], A. Manz[99], A. Mapelli[29], L. Mapelli[29], L. March [80], J.F. Marchand[29], F. Marchese[133a,133b], G. Marchiori[78], M. Marcisovsky[125], A. Marin[21,*], C.P. Marino[61], F. Marroquim[23a], R. Marshall[82], Z. Marshall[29], F.K. Martens[158], S. Marti-Garcia[167], A.J. Martin[175], B. Martin[29], B. Martin[88], F.F. Martin[120], J.P. Martin[93], Ph. Martin[55], T.A. Martin[17], B. Martin dit Latour[49], M. Martinez[11], V. Martinez Outschoorn[57], A.C. Martyniuk[82], M. Marx[82], F. Marzano[132a], A. Marzin[111], L. Masetti[81], T. Mashimo[155], R. Mashinistov[94], J. Masik[82], A.L. Maslennikov[107], M. Maß[42], I. Massa[19a,19b], G. Massaro[105], N. Massol[4], P. Mastrandrea[132a,132b], A. Mastroberardino[36a,36b], T. Masubuchi[155], M. Mathes[20], P. Matricon[115], H. Matsumoto[155], H. Matsunaga[155], T. Matsushita[67], C. Mattravers[118,c], J.M. Maugain[29], S.J. Maxfield[73], D.A. Maximov[107], E.N. May[5], A. Mayne[139], R. Mazini[151], M. Mazur[20], M. Mazzanti[89a], E. Mazzoni[122a,122b], S.P. Mc Kee[87], A. McCarn[165], R.L. McCarthy[148], T.G. McCarthy[28], N.A. McCubbin[129], K.W. McFarlane[56], J.A. Mcfayden[139], H. McGlone[53], G. Mchedlidze[51], R.A. McLaren[29], T. Mclaughlan[17], S.J. McMahon[129], R.A. McPherson[169,j], A. Meade[84], J. Mechnich[105], M. Mechtel[174], M. Medinnis[41], R. Meera-Lebbai[111], T. Meguro[116], R. Mehdiyev[93], S. Mehlhase[35], A. Mehta[73], K. Meier[58a], J. Meinhardt[48], B. Meirose[79], C. Melachrinos[30], B.R. Mellado Garcia[172], L. Mendoza Navas[162], Z. Meng[151,s], A. Mengarelli[19a,19b],

S. Menke[99], C. Menot[29], E. Meoni[11], K.M. Mercurio[57], P. Mermod[118], L. Merola[102a,102b], C. Meroni[89a], F.S. Merritt[30], A. Messina[29], J. Metcalfe[103], A.S. Mete[64], S. Meuser[20], C. Meyer[81], J-P. Meyer[136], J. Meyer[173], J. Meyer[54], T.C. Meyer[29], W.T. Meyer[64], J. Miao[32d], S. Michal[29], L. Micu[25a], R.P. Middleton[129], P. Miele[29], S. Migas[73], L. Mijović[41], G. Mikenberg[171], M. Mikestikova[125], M. Mikuž[74], D.W. Miller[143], R.J. Miller[88], W.J. Mills[168], C. Mills[57], A. Milov[171], D.A. Milstead[146a,146b], D. Milstein[171], A.A. Minaenko[128], M. Miñano[167], I.A. Minashvili[65], A.I. Mincer[108], B. Mindur[37], M. Mineev[65], Y. Ming[130], L.M. Mir[11], G. Mirabelli[132a], L. Miralles Verge[11], A. Misiejuk[76], J. Mitrevski[137], G.Y. Mitrofanov[128], V.A. Mitsou[167], S. Mitsui[66], P.S. Miyagawa[82], K. Miyazaki[67], J.U. Mjörnmark[79], T. Moa[146a,146b], P. Mockett[138], S. Moed[57], V. Moeller[27], K. Mönig[41], N. Möser[20], S. Mohapatra[148], B. Mohn[13], W. Mohr[48], S. Mohrdieck-Möck[99], A.M. Moisseev[128,*], R. Moles-Valls[167], J. Molina-Perez[29], J. Monk[77], E. Monnier[83], S. Montesano[89a,89b], F. Monticelli[70], S. Monzani[19a,19b], R.W. Moore[2], G.F. Moorhead[86], C. Mora Herrera[49], A. Moraes[53], A. Morais[124a,b], N. Morange[136], J. Morel[54], G. Morello[36a,36b], D. Moreno[81], M. Moreno Llácer[167], P. Morettini[50a], M. Morii[57], J. Morin[75], Y. Morita[66], A.K. Morley[29], G. Mornacchi[29], M-C. Morone[49], S.V. Morozov[96], J.D. Morris[75], L. Morvaj[101], H.G. Moser[99], M. Mosidze[51], J. Moss[109], R. Mount[143], E. Mountricha[136], S.V. Mouraviev[94], E.J.W. Moyse[84], M. Mudrinic[12b], F. Mueller[58a], J. Mueller[123], K. Mueller[20], T.A. Müller[98], D. Muenstermann[29], A. Muijs[105], A. Muir[168], Y. Munwes[153], K. Murakami[66], W.J. Murray[129], I. Mussche[105], E. Musto[102a,102b], A.G. Myagkov[128], M. Myska[125], J. Nadal[11], K. Nagai[160], K. Nagano[66], Y. Nagasaka[60], A.M. Nairz[29], Y. Nakahama[29], K. Nakamura[155], I. Nakano[110], G. Nanava[20], A. Napier[161], M. Nash[77,c], N.R. Nation[21], T. Nattermann[20], T. Naumann[41], G. Navarro[162], H.A. Neal[87], E. Nebot[80], P.Yu. Nechaeva[94], A. Negri[119a,119b], G. Negri[29], S. Nektarijevic[49], A. Nelson[64], S. Nelson[143], T.K. Nelson[143], S. Nemecek[125], P. Nemethy[108], A.A. Nepomuceno[23a], M. Nessi[29,u], S.Y. Nesterov[121], M.S. Neubauer[165], A. Neusiedl[81], R.M. Neves[108], P. Nevski[24], P.R. Newman[17], R.B. Nickerson[118], R. Nicolaidou[136], L. Nicolas[139], B. Nicquevert[29], F. Niedercorn[115], J. Nielsen[137], T. Niinikoski[29], A. Nikiforov[15], V. Nikolaenko[128], K. Nikolaev[65], I. Nikolic-Audit[78], K. Nikolopoulos[24], H. Nilsen[48], P. Nilsson[7], Y. Ninomiya [155], A. Nisati[132a], T. Nishiyama[67], R. Nisius[99], L. Nodulman[5], M. Nomachi[116], I. Nomidis[154], H. Nomoto[155], M. Nordberg[29], B. Nordkvist[146a,146b], P.R. Norton[129], J. Novakova[126], M. Nozaki[66], M. Nožička[41], L. Nozka[113], I.M. Nugent[159a], A.-E. Nuncio-Quiroz[20], G. Nunes Hanninger[20], T. Nunnemann[98], E. Nurse[77], T. Nyman[29], B.J. O'Brien[45], S.W. O'Neale[17,*], D.C. O'Neil[142], V. O'Shea[53], F.G. Oakham[28,e], H. Oberlack[99], J. Ocariz[78], A. Ochi[67], S. Oda[155], S. Odaka[66], J. Odier[83], H. Ogren[61], A. Oh[82], S.H. Oh[44], C.C. Ohm[146a,146b], T. Ohshima[101], H. Ohshita[140], T.K. Ohska[66], T. Ohsugi[59], S. Okada[67], H. Okawa[163], Y. Okumura[101], T. Okuyama[155], M. Olcese[50a], A.G. Olchevski[65], M. Oliveira[124a,h], D. Oliveira Damazio[24], E. Oliver Garcia[167], D. Olivito[120], A. Olszewski[38], J. Olszowska[38], C. Omachi[67], A. Onofre[124a,v], P.U.E. Onyisi[30], C.J. Oram[159a], M.J. Oreglia[30], Y. Oren[153], D. Orestano[134a,134b], I. Orlov[107], C. Oropeza Barrera[53], R.S. Orr[158], E.O. Ortega[130], B. Osculati[50a,50b], R. Ospanov[120], C. Osuna[11], G. Otero y Garzon[26],

J.P Ottersbach[105], M. Ouchrif[135d], F. Ould-Saada[117], A. Ouraou[136], Q. Ouyang[32a], M. Owen[82], S. Owen[139], O.K. Øye[13], V.E. Ozcan[18a], N. Ozturk[7], A. Pacheco Pages[11], C. Padilla Aranda[11], E. Paganis[139], F. Paige[24], K. Pajchel[117], S. Palestini[29], D. Pallin[33], A. Palma[124a,b], J.D. Palmer[17], Y.B. Pan[172], E. Panagiotopoulou[9], B. Panes[31a], N. Panikashvili[87], S. Panitkin[24], D. Pantea[25a], M. Panuskova[125], V. Paolone[123], A. Papadelis[146a], Th.D. Papadopoulou[9], A. Paramonov[5], W. Park[24,w], M.A. Parker[27], F. Parodi[50a,50b], J.A. Parsons[34], U. Parzefall[48], E. Pasqualucci[132a], A. Passeri[134a], F. Pastore[134a,134b], Fr. Pastore[29], G. Pásztor [49,x], S. Pataraia[172], N. Patel[150], J.R. Pater[82], S. Patricelli[102a,102b], T. Pauly[29], M. Pecsy[144a], M.I. Pedraza Morales[172], S.V. Peleganchuk[107], H. Peng[172], R. Pengo[29], A. Penson[34], J. Penwell[61], M. Perantoni[23a], K. Perez[34,t], T. Perez Cavalcanti[41], E. Perez Codina[11], M.T. Pérez García-Estañ[167], V. Perez Reale[34], I. Peric[20], L. Perini[89a,89b], H. Pernegger[29], R. Perrino[72a], P. Perrodo[4], S. Persembe[3a], V.D. Peshekhonov[65], O. Peters[105], B.A. Petersen[29], J. Petersen[29], T.C. Petersen[35], E. Petit[83], A. Petridis[154], C. Petridou[154], E. Petrolo[132a], F. Petrucci[134a,134b], D. Petschull[41], M. Petteni[142], R. Pezoa[31b], A. Phan[86], A.W. Phillips[27], P.W. Phillips[129], G. Piacquadio[29], E. Piccaro[75], M. Piccinini[19a,19b], A. Pickford[53], S.M. Piec[41], R. Piegaia[26], J.E. Pilcher[30], A.D. Pilkington[82], J. Pina[124a,b], M. Pinamonti[164a,164c], A. Pinder[118], J.L. Pinfold[2], J. Ping[32c], B. Pinto[124a,b], O. Pirotte[29], C. Pizio[89a,89b], R. Placakyte[41], M. Plamondon[169], W.G. Plano[82], M.-A. Pleier[24], A.V. Pleskach[128], A. Poblaguev[24], S. Poddar[58a], F. Podlyski[33], L. Poggioli[115], T. Poghosyan[20], M. Pohl[49], F. Polci[55], G. Polesello[119a], A. Policicchio[138], A. Polini[19a], J. Poll[75], V. Polychronakos[24], D.M. Pomarede[136], D. Pomeroy[22], K. Pommès[29], L. Pontecorvo[132a], B.G. Pope[88], G.A. Popeneciu[25a], D.S. Popovic[12a], A. Poppleton[29], X. Portell Bueso[48], R. Porter[163], C. Posch[21], G.E. Pospelov[99], S. Pospisil[127], I.N. Potrap[99], C.J. Potter[149], C.T. Potter[114], G. Poulard[29], J. Poveda[172], R. Prabhu[77], P. Pralavorio[83], S. Prasad[57], R. Pravahan[7], S. Prell[64], K. Pretzl[16], L. Pribyl[29], D. Price[61], L.E. Price[5], M.J. Price[29], P.M. Prichard[73], D. Prieur[123], M. Primavera[72a], K. Prokofiev[108], F. Prokoshin[31b], S. Protopopescu[24], J. Proudfoot[5], X. Prudent[43], H. Przysiezniak[4], S. Psoroulas[20], E. Ptacek[114], J. Purdham[87], M. Purohit[24,w], P. Puzo[115], Y. Pylypchenko[117], J. Qian[87], Z. Qian[83], Z. Qin[41], A. Quadt[54], D.R. Quarrie[14], W.B. Quayle[172], F. Quinonez[31a], M. Raas[104], V. Radescu[58b], B. Radics[20], T. Rador[18a], F. Ragusa[89a,89b], G. Rahal[177], A.M. Rahimi[109], D. Rahm[24], S. Rajagopalan[24], M. Rammensee[48], M. Rammes[141], M. Ramstedt[146a,146b], K. Randrianarivony[28], P.N. Ratoff[71], F. Rauscher[98], E. Rauter[99], M. Raymond[29], A.L. Read[117], D.M. Rebuzzi[119a,119b], A. Redelbach[173], G. Redlinger[24], R. Reece[120], K. Reeves[40], A. Reichold[105], E. Reinherz-Aronis[153], A. Reinsch[114], I. Reisinger[42], D. Reljic[12a], C. Rembser[29], Z.L. Ren[151], A. Renaud[115], P. Renkel[39], B. Rensch[35], M. Rescigno[132a], S. Resconi[89a], B. Resende[136], P. Reznicek[98], R. Rezvani[158], A. Richards[77], R. Richter[99], E. Richter-Was[38,y], M. Ridel[78], S. Rieke[81], M. Rijpstra[105], M. Rijssenbeek[148], A. Rimoldi[119a,119b], L. Rinaldi[19a], R.R. Rios[39], I. Riu[11], G. Rivoltella[89a,89b], F. Rizatdinova[112], E. Rizvi[75], S.H. Robertson[85,j], A. Robichaud-Veronneau[49], D. Robinson[27], J.E.M. Robinson[77], M. Robinson[114], A. Robson[53], J.G. Rocha de Lima[106], C. Roda[122a,122b], D. Roda Dos Santos[29], S. Rodier[80], D. Rodriguez[162],

Y. Rodriguez Garcia[15], A. Roe[54], S. Roe[29], O. Røhne[117], V. Rojo[1], S. Rolli[161], A. Romaniouk[96], V.M. Romanov[65], G. Romeo[26], D. Romero Maltrana[31a], L. Roos[78], E. Ros[167], S. Rosati[132a,132b], K. Rosbach[49], M. Rose[76], G.A. Rosenbaum[158], E.I. Rosenberg[64], P.L. Rosendahl[13], L. Rosselet[49], V. Rossetti[11], E. Rossi[102a,102b], L.P. Rossi[50a], L. Rossi[89a,89b], M. Rotaru[25a], I. Roth[171], J. Rothberg[138], D. Rousseau[115], C.R. Royon[136], A. Rozanov[83], Y. Rozen[152], X. Ruan[115], I. Rubinskiy[41], B. Ruckert[98], N. Ruckstuhl[105], V.I. Rud[97], G. Rudolph[62], F. Rühr[6], F. Ruggieri[134a,134b], A. Ruiz-Martinez[64], E. Rulikowska-Zarebska[37], V. Rumiantsev[91,*], L. Rumyantsev[65], K. Runge[48], O. Runolfsson[20], Z. Rurikova[48], N.A. Rusakovich[65], D.R. Rust[61], J.P. Rutherfoord[6], C. Ruwiedel[14], P. Ruzicka[125], Y.F. Ryabov[121], V. Ryadovikov[128], P. Ryan[88], M. Rybar[126], G. Rybkin[115], N.C. Ryder[118], S. Rzaeva[10], A.F. Saavedra[150], I. Sadeh[153], H.F-W. Sadrozinski[137], R. Sadykov[65], F. Safai Tehrani[132a,132b], H. Sakamoto[155], G. Salamanna[75], A. Salamon[133a], M. Saleem[111], D. Salihagic[99], A. Salnikov[143], J. Salt[167], B.M. Salvachua Ferrando[5], D. Salvatore[36a,36b], F. Salvatore[149], A. Salvucci[104], A. Salzburger[29], D. Sampsonidis[154], B.H. Samset[117], H. Sandaker[13], H.G. Sander[81], M.P. Sanders[98], M. Sandhoff[174], T. Sandoval[27], R. Sandstroem[99], S. Sandvoss[174], D.P.C. Sankey[129], A. Sansoni[47], C. Santamarina Rios[85], C. Santoni[33], R. Santonico[133a,133b], H. Santos[124a], J.G. Saraiva[124a,b], T. Sarangi[172], E. Sarkisyan-Grinbaum[7], F. Sarri[122a,122b], G. Sartisohn[174], O. Sasaki[66], T. Sasaki[66], N. Sasao[68], I. Satsounkevitch[90], G. Sauvage[4], J.B. Sauvan[115], P. Savard[158,e], V. Savinov[123], D.O. Savu[29], P. Savva [9], L. Sawyer[24,l], D.H. Saxon[53], L.P. Says[33], C. Sbarra[19a,19b], A. Sbrizzi[19a,19b], O. Scallon[93], D.A. Scannicchio[163], J. Schaarschmidt[115], P. Schacht[99], U. Schäfer[81], S. Schaepe[20], S. Schaetzel[58b], A.C. Schaffer[115], D. Schaile[98], R.D. Schamberger[148], A.G. Schamov[107], V. Scharf[58a], V.A. Schegelsky[121], D. Scheirich[87], M.I. Scherzer[14], C. Schiavi[50a,50b], J. Schieck[98], M. Schioppa[36a,36b], S. Schlenker[29], J.L. Schlereth[5], E. Schmidt[48], M.P. Schmidt[175,*], K. Schmieden[20], C. Schmitt[81], S. Schmitt[58b], M. Schmitz[20], A. Schöning[58b], M. Schott[29], D. Schouten[142], J. Schovancova[125], M. Schram[85], C. Schroeder[81], N. Schroer[58c], S. Schuh[29], G. Schuler[29], J. Schultes[174], H.-C. Schultz-Coulon[58a], H. Schulz[15], J.W. Schumacher[20], M. Schumacher[48], B.A. Schumm[137], Ph. Schune[136], C. Schwanenberger[82], A. Schwartzman[143], Ph. Schwemling[78], R. Schwienhorst[88], R. Schwierz[43], J. Schwindling[136], W.G. Scott[129], J. Searcy[114], E. Sedykh[121], E. Segura[11], S.C. Seidel[103], A. Seiden[137], F. Seifert[43], J.M. Seixas[23a], G. Sekhniaidze[102a], D.M. Seliverstov[121], B. Sellden[146a], G. Sellers[73], M. Seman[144b], N. Semprini-Cesari[19a,19b], C. Serfon[98], L. Serin[115], R. Seuster[99], H. Severini[111], M.E. Sevior[86], A. Sfyrla[29], E. Shabalina[54], M. Shamim[114], L.Y. Shan[32a], J.T. Shank[21], Q.T. Shao[86], M. Shapiro[14], P.B. Shatalov[95], L. Shaver[6], C. Shaw[53], K. Shaw[164a,164c], D. Sherman[175], P. Sherwood[77], A. Shibata[108], H. Shichi[101], S. Shimizu[29], M. Shimojima[100], T. Shin[56], A. Shmeleva[94], M.J. Shochet[30], D. Short[118], M.A. Shupe[6], P. Sicho[125], A. Sidoti[132a,132b], A. Siebel[174], F. Siegert[48], J. Siegrist[14], Dj. Sijacki[12a], O. Silbert[171], J. Silva[124a,b], Y. Silver[153], D. Silverstein[143], S.B. Silverstein[146a], V. Simak[127], O. Simard[136], Lj. Simic[12a], S. Simion[115], B. Simmons[77], M. Simonyan[35], P. Sinervo[158], N.B. Sinev[114], V. Sipica[141], G. Siragusa[81], A.N. Sisakyan[65], S.Yu. Sivoklokov[97], J. Sjölin[146a,146b], T.B. Sjursen[13], L.A. Skinnari[14],

K. Skovpen[107], P. Skubic[111], N. Skvorodnev[22], M. Slater[17], T. Slavicek[127], K. Sliwa[161], T.J. Sloan[71], J. Sloper[29], V. Smakhtin[171], S.Yu. Smirnov[96], L.N. Smirnova[97], O. Smirnova[79], B.C. Smith[57], D. Smith[143], K.M. Smith[53], M. Smizanska[71], K. Smolek[127], A.A. Snesarev[94], S.W. Snow[82], J. Snow[111], J. Snuverink[105], S. Snyder[24], M. Soares[124a], R. Sobie[169,j], J. Sodomka[127], A. Soffer[153], C.A. Solans[167], M. Solar[127], J. Solc[127], E. Soldatov[96], U. Soldevila[167], E. Solfaroli Camillocci[132a,132b], A.A. Solodkov[128], O.V. Solovyanov[128], J. Sondericker[24], N. Soni[2], V. Sopko[127], B. Sopko[127], M. Sorbi[89a,89b], M. Sosebee[7], A. Soukharev[107], S. Spagnolo[72a,72b], F. Spanò[34], R. Spighi[19a], G. Spigo[29], F. Spila[132a,132b], E. Spiriti[134a], R. Spiwoks[29], M. Spousta[126], T. Spreitzer[158], B. Spurlock[7], R.D. St. Denis[53], T. Stahl[141], J. Stahlman[120], R. Stamen[58a], E. Stanecka[29], R.W. Stanek[5], C. Stanescu[134a], S. Stapnes[117], E.A. Starchenko[128], J. Stark[55], P. Staroba[125], P. Starovoitov[91], A. Staude[98], P. Stavina[144a], G. Stavropoulos[14], G. Steele[53], P. Steinbach[43], P. Steinberg[24], I. Stekl[127], B. Stelzer[142], H.J. Stelzer[41], O. Stelzer-Chilton[159a], H. Stenzel[52], K. Stevenson[75], G.A. Stewart[29], J.A. Stillings[20], T. Stockmanns[20], M.C. Stockton[29], K. Stoerig[48], G. Stoicea[25a], S. Stonjek[99], P. Strachota[126], A.R. Stradling[7], A. Straessner[43], J. Strandberg[147], S. Strandberg[146a,146b], A. Strandlie[117], M. Strang[109], E. Strauss[143], M. Strauss[111], P. Strizenec[144b], R. Ströhmer[173], D.M. Strom[114], J.A. Strong[76,*], R. Stroynowski[39], J. Strube[129], B. Stugu[13], I. Stumer[24,*], J. Stupak[148], P. Sturm[174], D.A. Soh[151,q], D. Su[143], HS. Subramania[2], A. Succurro[11], Y. Sugaya[116], T. Sugimoto[101], C. Suhr[106], K. Suita[67], M. Suk[126], V.V. Sulin[94], S. Sultansoy[3d], T. Sumida[29], X. Sun[55], J.E. Sundermann[48], K. Suruliz[139], S. Sushkov[11], G. Susinno[36a,36b], M.R. Sutton[149], Y. Suzuki[66], M. Svatos[125], Yu.M. Sviridov[128], S. Swedish[168], I. Sykora[144a], T. Sykora[126], B. Szeless[29], J. Sánchez[167], D. Ta[105], K. Tackmann[41], A. Taffard[163], R. Tafirout[159a], A. Taga[117], N. Taiblum[153], Y. Takahashi[101], H. Takai[24], R. Takashima[69], H. Takeda[67], T. Takeshita[140], M. Talby[83], A. Talyshev[107], M.C. Tamsett[24], J. Tanaka[155], R. Tanaka[115], S. Tanaka[131], S. Tanaka[66], Y. Tanaka[100], K. Tani[67], N. Tannoury[83], G.P. Tappern[29], S. Tapprogge[81], D. Tardif[158], S. Tarem[152], F. Tarrade[24], G.F. Tartarelli[89a], P. Tas[126], M. Tasevsky[125], E. Tassi[36a,36b], M. Tatarkhanov[14], C. Taylor[77], F.E. Taylor[92], G.N. Taylor[86], W. Taylor[159b], M. Teixeira Dias Castanheira[75], P. Teixeira-Dias[76], K.K. Temming[48], H. Ten Kate[29], P.K. Teng[151], S. Terada[66], K. Terashi[155], J. Terron[80], M. Terwort[41,o], M. Testa[47], R.J. Teuscher[158,j], J. Thadome[174], J. Therhaag[20], T. Theveneaux-Pelzer[78], M. Thioye[175], S. Thoma[48], J.P. Thomas[17], E.N. Thompson[84], P.D. Thompson[17], P.D. Thompson[158], A.S. Thompson[53], E. Thomson[120], M. Thomson[27], R.P. Thun[87], T. Tic[125], V.O. Tikhomirov[94], Y.A. Tikhonov[107], C.J.W.P. Timmermans[104], P. Tipton[175], F.J. Tique Aires Viegas[29], S. Tisserant[83], J. Tobias[48], B. Toczek[37], T. Todorov[4], S. Todorova-Nova[161], B. Toggerson[163], J. Tojo[66], S. Tokár[144a], K. Tokunaga[67], K. Tokushuku[66], K. Tollefson[88], M. Tomoto[101], L. Tompkins[14], K. Toms[103], G. Tong[32a], A. Tonoyan[13], C. Topfel[16], N.D. Topilin[65], I. Torchiani[29], E. Torrence[114], E. Torró Pastor[167], J. Toth[83,x], F. Touchard[83], D.R. Tovey[139], D. Traynor[75], T. Trefzger[173], J. Treis[20], L. Tremblet[29], A. Tricoli[29], I.M. Trigger[159a], S. Trincaz-Duvoid[78], T.N. Trinh[78], M.F. Tripiana[70], W. Trischuk[158], A. Trivedi[24,w], B. Trocmé[55], C. Troncon[89a], M. Trottier-McDonald[142], A. Trzupek[38], C. Tsarouchas[29],

J.C-L. Tseng[118], M. Tsiakiris[105], P.V. Tsiareshka[90], D. Tsionou[4], G. Tsipolitis[9], V. Tsiskaridze[48], E.G. Tskhadadze[51], I.I. Tsukerman[95], V. Tsulaia[123], J.-W. Tsung[20], S. Tsuno[66], D. Tsybychev[148], A. Tua[139], J.M. Tuggle[30], M. Turala[38], D. Turecek[127], I. Turk Cakir[3e], E. Turlay[105], R. Turra[89a,89b], P.M. Tuts[34], A. Tykhonov[74], M. Tylmad[146a,146b], M. Tyndel[129], H. Tyrvainen[29], G. Tzanakos[8], K. Uchida[20], I. Ueda[155], R. Ueno[28], M. Ugland[13], M. Uhlenbrock[20], M. Uhrmacher[54], F. Ukegawa[160], G. Unal[29], D.G. Underwood[5], A. Undrus[24], G. Unel[163], Y. Unno[66], D. Urbaniec[34], E. Urkovsky[153], P. Urrejola[31a], G. Usai[7], M. Uslenghi[119a,119b], L. Vacavant[83], V. Vacek[127], B. Vachon[85], S. Vahsen[14], J. Valenta[125], P. Valente[132a], S. Valentinetti[19a,19b], S. Valkar[126], E. Valladolid Gallego[167], S. Vallecorsa[152], J.A. Valls Ferrer[167], H. van der Graaf[105], E. van der Kraaij[105], R. Van Der Leeuw[105], E. van der Poel[105], D. van der Ster[29], B. Van Eijk[105], N. van Eldik[84], P. van Gemmeren[5], Z. van Kesteren[105], I. van Vulpen[105], W. Vandelli[29], G. Vandoni[29], A. Vaniachine[5], P. Vankov[41], F. Vannucci[78], F. Varela Rodriguez[29], R. Vari[132a], E.W. Varnes[6], D. Varouchas[14], A. Vartapetian[7], K.E. Varvell[150], V.I. Vassilakopoulos[56], F. Vazeille[33], G. Vegni[89a,89b], J.J. Veillet[115], C. Vellidis[8], F. Veloso[124a], R. Veness[29], S. Veneziano[132a], A. Ventura[72a,72b], D. Ventura[138], M. Venturi[48], N. Venturi[16], V. Vercesi[119a], M. Verducci[138], W. Verkerke[105], J.C. Vermeulen[105], A. Vest[43], M.C. Vetterli[142,e], I. Vichou[165], T. Vickey[145b,z], G.H.A. Viehhauser[118], S. Viel[168], M. Villa[19a,19b], M. Villaplana Perez[167], E. Vilucchi[47], M.G. Vincter[28], E. Vinek[29], V.B. Vinogradov[65], M. Virchaux[136,*], S. Viret[33], J. Virzi[14], A. Vitale [19a,19b], O. Vitells[171], M. Viti[41], I. Vivarelli[48], F. Vives Vaque[11], S. Vlachos[9], M. Vlasak[127], N. Vlasov[20], A. Vogel[20], P. Vokac[127], G. Volpi[47], M. Volpi[11], G. Volpini[89a], H. von der Schmitt[99], J. von Loeben[99], H. von Radziewski[48], E. von Toerne[20], V. Vorobel[126], A.P. Vorobiev[128], V. Vorwerk[11], M. Vos[167], R. Voss[29], T.T. Voss[174], J.H. Vossebeld[73], N. Vranjes[12a], M. Vranjes Milosavljevic[12a], V. Vrba[125], M. Vreeswijk[105], T. Vu Anh[81], R. Vuillermet[29], I. Vukotic[115], W. Wagner[174], P. Wagner[120], H. Wahlen[174], J. Wakabayashi[101], J. Walbersloh[42], S. Walch[87], J. Walder[71], R. Walker[98], W. Walkowiak[141], R. Wall[175], P. Waller[73], C. Wang[44], H. Wang[172], H. Wang[32b,aa], J. Wang[151], J. Wang[32d], J.C. Wang[138], R. Wang[103], S.M. Wang[151], A. Warburton[85], C.P. Ward[27], M. Warsinsky[48], P.M. Watkins[17], A.T. Watson[17], M.F. Watson[17], G. Watts[138], S. Watts[82], A.T. Waugh[150], B.M. Waugh[77], J. Weber[42], M. Weber[129], M.S. Weber[16], P. Weber[54], A.R. Weidberg[118], P. Weigell[99], J. Weingarten[54], C. Weiser[48], H. Wellenstein[22], P.S. Wells[29], M. Wen[47], T. Wenaus[24], S. Wendler[123], Z. Weng[151,q], T. Wengler[29], S. Wenig[29], N. Wermes[20], M. Werner[48], P. Werner[29], M. Werth[163], M. Wessels[58a], C. Weydert[55], K. Whalen[28], S.J. Wheeler-Ellis[163], S.P. Whitaker[21], A. White[7], M.J. White[86], S. White[24], S.R. Whitehead[118], D. Whiteson[163], D. Whittington[61], F. Wicek[115], D. Wicke[174], F.J. Wickens[129], W. Wiedenmann[172], M. Wielers[129], P. Wienemann[20], C. Wiglesworth[75], L.A.M. Wiik[48], P.A. Wijeratne[77], A. Wildauer[167], M.A. Wildt[41,o], I. Wilhelm[126], H.G. Wilkens[29], J.Z. Will[98], E. Williams[34], H.H. Williams[120], W. Willis[34], S. Willocq[84], J.A. Wilson[17], M.G. Wilson[143], A. Wilson[87], I. Wingerter-Seez[4], S. Winkelmann[48], F. Winklmeier[29], M. Wittgen[143], M.W. Wolter[38], H. Wolters[124a,h], G. Wooden[118], B.K. Wosiek[38], J. Wotschack[29], M.J. Woudstra[84],

K. Wraight[53], C. Wright[53], B. Wrona[73], S.L. Wu[172], X. Wu[49], Y. Wu[32b,ab], E. Wulf[34], R. Wunstorf[42], B.M. Wynne[45], L. Xaplanteris[9], S. Xella[35], S. Xie[48], Y. Xie[32a], C. Xu[32b,ac], D. Xu[139], G. Xu[32a], B. Yabsley[150], M. Yamada[66], A. Yamamoto[66], K. Yamamoto[64], S. Yamamoto[155], T. Yamamura[155], J. Yamaoka[44], T. Yamazaki[155], Y. Yamazaki[67], Z. Yan[21], H. Yang[87], U.K. Yang[82], Y. Yang[61], Y. Yang[32a], Z. Yang[146a,146b], S. Yanush[91], W-M. Yao[14], Y. Yao[14], Y. Yasu[66], G.V. Ybeles Smit[130], J. Ye[39], S. Ye[24], M. Yilmaz[3c], R. Yoosoofmiya[123], K. Yorita[170], R. Yoshida[5], C. Young[143], S. Youssef[21], D. Yu[24], J. Yu[7], J. Yu[32c,ac], L. Yuan[32a,ad], A. Yurkewicz[148], V.G. Zaets [128], R. Zaidan[63], A.M. Zaitsev[128], Z. Zajacova[29], Yo.K. Zalite [121], L. Zanello[132a,132b], P. Zarzhitsky[39], A. Zaytsev[107], C. Zeitnitz[174], M. Zeller[175], A. Zemla[38], C. Zendler[20], A.V. Zenin[128], O. Zenin[128], T. Ženiš[144a], Z. Zenonos[122a,122b], S. Zenz[14], D. Zerwas[115], G. Zevi della Porta[57], Z. Zhan[32d], D. Zhang[32b,aa], H. Zhang[88], J. Zhang[5], X. Zhang[32d], Z. Zhang[115], L. Zhao[108], T. Zhao[138], Z. Zhao[32b], A. Zhemchugov[65], S. Zheng[32a], J. Zhong[151,ae], B. Zhou[87], N. Zhou[163], Y. Zhou[151], C.G. Zhu[32d], H. Zhu[41], Y. Zhu[172], X. Zhuang[98], V. Zhuravlov[99], D. Zieminska[61], R. Zimmermann[20], S. Zimmermann[20], S. Zimmermann[48], M. Ziolkowski[141], R. Zitoun[4], L. Živković[34], V.V. Zmouchko[128,*], G. Zobernig[172], A. Zoccoli[19a,19b], Y. Zolnierowski[4], A. Zsenei[29], M. zur Nedden[15], V. Zutshi[106], L. Zwalinski[29].

[1] University at Albany, Albany NY, United States of America
[2] Department of Physics, University of Alberta, Edmonton AB, Canada
[3] [(a)]Department of Physics, Ankara University, Ankara; [(b)]Department of Physics, Dumlupinar University, Kutahya; [(c)]Department of Physics, Gazi University, Ankara; [(d)]Division of Physics, TOBB University of Economics and Technology, Ankara; [(e)]Turkish Atomic Energy Authority, Ankara, Turkey
[4] LAPP, CNRS/IN2P3 and Université de Savoie, Annecy-le-Vieux, France
[5] High Energy Physics Division, Argonne National Laboratory, Argonne IL, United States of America
[6] Department of Physics, University of Arizona, Tucson AZ, United States of America
[7] Department of Physics, The University of Texas at Arlington, Arlington TX, United States of America
[8] Physics Department, University of Athens, Athens, Greece
[9] Physics Department, National Technical University of Athens, Zografou, Greece
[10] Institute of Physics, Azerbaijan Academy of Sciences, Baku, Azerbaijan
[11] Institut de Física d'Altes Energies and Universitat Autònoma de Barcelona and ICREA, Barcelona, Spain
[12] [(a)]Institute of Physics, University of Belgrade, Belgrade; [(b)]Vinca Institute of Nuclear Sciences, Belgrade, Serbia
[13] Department for Physics and Technology, University of Bergen, Bergen, Norway
[14] Physics Division, Lawrence Berkeley National Laboratory and University of California, Berkeley CA, United States of America
[15] Department of Physics, Humboldt University, Berlin, Germany
[16] Albert Einstein Center for Fundamental Physics and Laboratory for High Energy

Physics, University of Bern, Bern, Switzerland
[17] School of Physics and Astronomy, University of Birmingham, Birmingham, United Kingdom
[18] [(a)]Department of Physics, Bogazici University, Istanbul; [(b)]Division of Physics, Dogus University, Istanbul; [(c)]Department of Physics Engineering, Gaziantep University, Gaziantep; [(d)]Department of Physics, Istanbul Technical University, Istanbul, Turkey
[19] [(a)]INFN Sezione di Bologna; [(b)]Dipartimento di Fisica, Università di Bologna, Bologna, Italy
[20] Physikalisches Institut, University of Bonn, Bonn, Germany
[21] Department of Physics, Boston University, Boston MA, United States of America
[22] Department of Physics, Brandeis University, Waltham MA, United States of America
[23] [(a)]Universidade Federal do Rio De Janeiro COPPE/EE/IF, Rio de Janeiro; [(b)]Instituto de Fisica, Universidade de Sao Paulo, Sao Paulo, Brazil
[24] Physics Department, Brookhaven National Laboratory, Upton NY, United States of America
[25] [(a)]National Institute of Physics and Nuclear Engineering, Bucharest; [(b)]University Politehnica Bucharest, Bucharest; [(c)]West University in Timisoara, Timisoara, Romania
[26] Departamento de Física, Universidad de Buenos Aires, Buenos Aires, Argentina
[27] Cavendish Laboratory, University of Cambridge, Cambridge, United Kingdom
[28] Department of Physics, Carleton University, Ottawa ON, Canada
[29] CERN, Geneva, Switzerland
[30] Enrico Fermi Institute, University of Chicago, Chicago IL, United States of America
[31] [(a)]Departamento de Fisica, Pontificia Universidad Católica de Chile, Santiago; [(b)]Departamento de Física, Universidad Técnica Federico Santa María, Valparaíso, Chile
[32] [(a)]Institute of High Energy Physics, Chinese Academy of Sciences, Beijing; [(b)]Department of Modern Physics, University of Science and Technology of China, Anhui; [(c)]Department of Physics, Nanjing University, Jiangsu; [(d)]High Energy Physics Group, Shandong University, Shandong, China
[33] Laboratoire de Physique Corpusculaire, Clermont Université and Université Blaise Pascal and CNRS/IN2P3, Aubiere Cedex, France
[34] Nevis Laboratory, Columbia University, Irvington NY, United States of America
[35] Niels Bohr Institute, University of Copenhagen, Kobenhavn, Denmark
[36] [(a)]INFN Gruppo Collegato di Cosenza; [(b)]Dipartimento di Fisica, Università della Calabria, Arcavata di Rende, Italy
[37] Faculty of Physics and Applied Computer Science, AGH-University of Science and Technology, Krakow, Poland
[38] The Henryk Niewodniczanski Institute of Nuclear Physics, Polish Academy of Sciences, Krakow, Poland
[39] Physics Department, Southern Methodist University, Dallas TX, United States of America
[40] Physics Department, University of Texas at Dallas, Richardson TX, United States of America
[41] DESY, Hamburg and Zeuthen, Germany

[42] Institut für Experimentelle Physik IV, Technische Universität Dortmund, Dortmund, Germany
[43] Institut für Kern- und Teilchenphysik, Technical University Dresden, Dresden, Germany
[44] Department of Physics, Duke University, Durham NC, United States of America
[45] SUPA - School of Physics and Astronomy, University of Edinburgh, Edinburgh, United Kingdom
[46] Johannes Gutenbergstrasse 3 2700 Wiener Neustadt, Austria
[47] INFN Laboratori Nazionali di Frascati, Frascati, Italy
[48] Fakultät für Mathematik und Physik, Albert-Ludwigs-Universität, Freiburg i.Br., Germany
[49] Section de Physique, Université de Genève, Geneva, Switzerland
[50] [(a)]INFN Sezione di Genova; [(b)]Dipartimento di Fisica, Università di Genova, Genova, Italy
[51] Institute of Physics and HEP Institute, Georgian Academy of Sciences and Tbilisi State University, Tbilisi, Georgia
[52] II Physikalisches Institut, Justus-Liebig-Universität Giessen, Giessen, Germany
[53] SUPA - School of Physics and Astronomy, University of Glasgow, Glasgow, United Kingdom
[54] II Physikalisches Institut, Georg-August-Universität, Göttingen, Germany
[55] Laboratoire de Physique Subatomique et de Cosmologie, Université Joseph Fourier and CNRS/IN2P3 and Institut National Polytechnique de Grenoble, Grenoble, France
[56] Department of Physics, Hampton University, Hampton VA, United States of America
[57] Laboratory for Particle Physics and Cosmology, Harvard University, Cambridge MA, United States of America
[58] [(a)]Kirchhoff-Institut für Physik, Ruprecht-Karls-Universität Heidelberg, Heidelberg; [(b)]Physikalisches Institut, Ruprecht-Karls-Universität Heidelberg, Heidelberg; [(c)]ZITI Institut für technische Informatik, Ruprecht-Karls-Universität Heidelberg, Mannheim, Germany
[59] Faculty of Science, Hiroshima University, Hiroshima, Japan
[60] Faculty of Applied Information Science, Hiroshima Institute of Technology, Hiroshima, Japan
[61] Department of Physics, Indiana University, Bloomington IN, United States of America
[62] Institut für Astro- und Teilchenphysik, Leopold-Franzens-Universität, Innsbruck, Austria
[63] University of Iowa, Iowa City IA, United States of America
[64] Department of Physics and Astronomy, Iowa State University, Ames IA, United States of America
[65] Joint Institute for Nuclear Research, JINR Dubna, Dubna, Russia
[66] KEK, High Energy Accelerator Research Organization, Tsukuba, Japan
[67] Graduate School of Science, Kobe University, Kobe, Japan
[68] Faculty of Science, Kyoto University, Kyoto, Japan
[69] Kyoto University of Education, Kyoto, Japan

[70] Instituto de Física La Plata, Universidad Nacional de La Plata and CONICET, La Plata, Argentina
[71] Physics Department, Lancaster University, Lancaster, United Kingdom
[72] [(a)]INFN Sezione di Lecce; [(b)]Dipartimento di Fisica, Università del Salento, Lecce, Italy
[73] Oliver Lodge Laboratory, University of Liverpool, Liverpool, United Kingdom
[74] Department of Physics, Jožef Stefan Institute and University of Ljubljana, Ljubljana, Slovenia
[75] Department of Physics, Queen Mary University of London, London, United Kingdom
[76] Department of Physics, Royal Holloway University of London, Surrey, United Kingdom
[77] Department of Physics and Astronomy, University College London, London, United Kingdom
[78] Laboratoire de Physique Nucléaire et de Hautes Energies, UPMC and Université Paris-Diderot and CNRS/IN2P3, Paris, France
[79] Fysiska institutionen, Lunds universitet, Lund, Sweden
[80] Departamento de Fisica Teorica C-15, Universidad Autonoma de Madrid, Madrid, Spain
[81] Institut für Physik, Universität Mainz, Mainz, Germany
[82] School of Physics and Astronomy, University of Manchester, Manchester, United Kingdom
[83] CPPM, Aix-Marseille Université and CNRS/IN2P3, Marseille, France
[84] Department of Physics, University of Massachusetts, Amherst MA, United States of America
[85] Department of Physics, McGill University, Montreal QC, Canada
[86] School of Physics, University of Melbourne, Victoria, Australia
[87] Department of Physics, The University of Michigan, Ann Arbor MI, United States of America
[88] Department of Physics and Astronomy, Michigan State University, East Lansing MI, United States of America
[89] [(a)]INFN Sezione di Milano; [(b)]Dipartimento di Fisica, Università di Milano, Milano, Italy
[90] B.I. Stepanov Institute of Physics, National Academy of Sciences of Belarus, Minsk, Republic of Belarus
[91] National Scientific and Educational Centre for Particle and High Energy Physics, Minsk, Republic of Belarus
[92] Department of Physics, Massachusetts Institute of Technology, Cambridge MA, United States of America
[93] Group of Particle Physics, University of Montreal, Montreal QC, Canada
[94] P.N. Lebedev Institute of Physics, Academy of Sciences, Moscow, Russia
[95] Institute for Theoretical and Experimental Physics (ITEP), Moscow, Russia
[96] Moscow Engineering and Physics Institute (MEPhI), Moscow, Russia
[97] Skobeltsyn Institute of Nuclear Physics, Lomonosov Moscow State University, Moscow, Russia
[98] Fakultät für Physik, Ludwig-Maximilians-Universität München, München, Germany

[99] Max-Planck-Institut für Physik (Werner-Heisenberg-Institut), München, Germany
[100] Nagasaki Institute of Applied Science, Nagasaki, Japan
[101] Graduate School of Science, Nagoya University, Nagoya, Japan
[102] [(a)]INFN Sezione di Napoli; [(b)]Dipartimento di Scienze Fisiche, Università di Napoli, Napoli, Italy
[103] Department of Physics and Astronomy, University of New Mexico, Albuquerque NM, United States of America
[104] Institute for Mathematics, Astrophysics and Particle Physics, Radboud University Nijmegen/Nikhef, Nijmegen, Netherlands
[105] Nikhef National Institute for Subatomic Physics and University of Amsterdam, Amsterdam, Netherlands
[106] Department of Physics, Northern Illinois University, DeKalb IL, United States of America
[107] Budker Institute of Nuclear Physics (BINP), Novosibirsk, Russia
[108] Department of Physics, New York University, New York NY, United States of America
[109] Ohio State University, Columbus OH, United States of America
[110] Faculty of Science, Okayama University, Okayama, Japan
[111] Homer L. Dodge Department of Physics and Astronomy, University of Oklahoma, Norman OK, United States of America
[112] Department of Physics, Oklahoma State University, Stillwater OK, United States of America
[113] Palacký University, RCPTM, Olomouc, Czech Republic
[114] Center for High Energy Physics, University of Oregon, Eugene OR, United States of America
[115] LAL, Univ. Paris-Sud and CNRS/IN2P3, Orsay, France
[116] Graduate School of Science, Osaka University, Osaka, Japan
[117] Department of Physics, University of Oslo, Oslo, Norway
[118] Department of Physics, Oxford University, Oxford, United Kingdom
[119] [(a)]INFN Sezione di Pavia; [(b)]Dipartimento di Fisica Nucleare e Teorica, Università di Pavia, Pavia, Italy
[120] Department of Physics, University of Pennsylvania, Philadelphia PA, United States of America
[121] Petersburg Nuclear Physics Institute, Gatchina, Russia
[122] [(a)]INFN Sezione di Pisa; [(b)]Dipartimento di Fisica E. Fermi, Università di Pisa, Pisa, Italy
[123] Department of Physics and Astronomy, University of Pittsburgh, Pittsburgh PA, United States of America
[124] [(a)]Laboratorio de Instrumentacao e Fisica Experimental de Particulas - LIP, Lisboa, Portugal; [(b)]Departamento de Fisica Teorica y del Cosmos and CAFPE, Universidad de Granada, Granada, Spain
[125] Institute of Physics, Academy of Sciences of the Czech Republic, Praha, Czech Republic
[126] Faculty of Mathematics and Physics, Charles University in Prague, Praha, Czech

Republic
[127] Czech Technical University in Prague, Praha, Czech Republic
[128] State Research Center Institute for High Energy Physics, Protvino, Russia
[129] Particle Physics Department, Rutherford Appleton Laboratory, Didcot, United Kingdom
[130] Physics Department, University of Regina, Regina SK, Canada
[131] Ritsumeikan University, Kusatsu, Shiga, Japan
[132] [(a)]INFN Sezione di Roma I; [(b)]Dipartimento di Fisica, Università La Sapienza, Roma, Italy
[133] [(a)]INFN Sezione di Roma Tor Vergata; [(b)]Dipartimento di Fisica, Università di Roma Tor Vergata, Roma, Italy
[134] [(a)]INFN Sezione di Roma Tre; [(b)]Dipartimento di Fisica, Università Roma Tre, Roma, Italy
[135] [(a)]Faculté des Sciences Ain Chock, Réseau Universitaire de Physique des Hautes Energies - Université Hassan II, Casablanca; [(b)]Centre National de l'Energie des Sciences Techniques Nucleaires, Rabat; [(c)]Université Cadi Ayyad, Faculté des sciences Semlalia Département de Physique, B.P. 2390 Marrakech 40000; [(d)]Faculté des Sciences, Université Mohamed Premier and LPTPM, Oujda; [(e)]Faculté des Sciences, Université Mohammed V, Rabat, Morocco
[136] DSM/IRFU (Institut de Recherches sur les Lois Fondamentales de l'Univers), CEA Saclay (Commissariat a l'Energie Atomique), Gif-sur-Yvette, France
[137] Santa Cruz Institute for Particle Physics, University of California Santa Cruz, Santa Cruz CA, United States of America
[138] Department of Physics, University of Washington, Seattle WA, United States of America
[139] Department of Physics and Astronomy, University of Sheffield, Sheffield, United Kingdom
[140] Department of Physics, Shinshu University, Nagano, Japan
[141] Fachbereich Physik, Universität Siegen, Siegen, Germany
[142] Department of Physics, Simon Fraser University, Burnaby BC, Canada
[143] SLAC National Accelerator Laboratory, Stanford CA, United States of America
[144] [(a)]Faculty of Mathematics, Physics & Informatics, Comenius University, Bratislava; [(b)]Department of Subnuclear Physics, Institute of Experimental Physics of the Slovak Academy of Sciences, Kosice, Slovak Republic
[145] [(a)]Department of Physics, University of Johannesburg, Johannesburg; [(b)]School of Physics, University of the Witwatersrand, Johannesburg, South Africa
[146] [(a)]Department of Physics, Stockholm University; [(b)]The Oskar Klein Centre, Stockholm, Sweden
[147] Physics Department, Royal Institute of Technology, Stockholm, Sweden
[148] Department of Physics and Astronomy, Stony Brook University, Stony Brook NY, United States of America
[149] Department of Physics and Astronomy, University of Sussex, Brighton, United Kingdom

[150] School of Physics, University of Sydney, Sydney, Australia
[151] Institute of Physics, Academia Sinica, Taipei, Taiwan
[152] Department of Physics, Technion: Israel Inst. of Technology, Haifa, Israel
[153] Raymond and Beverly Sackler School of Physics and Astronomy, Tel Aviv University, Tel Aviv, Israel
[154] Department of Physics, Aristotle University of Thessaloniki, Thessaloniki, Greece
[155] International Center for Elementary Particle Physics and Department of Physics, The University of Tokyo, Tokyo, Japan
[156] Graduate School of Science and Technology, Tokyo Metropolitan University, Tokyo, Japan
[157] Department of Physics, Tokyo Institute of Technology, Tokyo, Japan
[158] Department of Physics, University of Toronto, Toronto ON, Canada
[159] [(a)]TRIUMF, Vancouver BC; [(b)]Department of Physics and Astronomy, York University, Toronto ON, Canada
[160] Institute of Pure and Applied Sciences, University of Tsukuba, Ibaraki, Japan
[161] Science and Technology Center, Tufts University, Medford MA, United States of America
[162] Centro de Investigaciones, Universidad Antonio Narino, Bogota, Colombia
[163] Department of Physics and Astronomy, University of California Irvine, Irvine CA, United States of America
[164] [(a)]INFN Gruppo Collegato di Udine; [(b)]ICTP, Trieste; [(c)]Dipartimento di Fisica, Università di Udine, Udine, Italy
[165] Department of Physics, University of Illinois, Urbana IL, United States of America
[166] Department of Physics and Astronomy, University of Uppsala, Uppsala, Sweden
[167] Instituto de Física Corpuscular (IFIC) and Departamento de Física Atómica, Molecular y Nuclear and Departamento de Ingenierá Electrónica and Instituto de Microelectrónica de Barcelona (IMB-CNM), University of Valencia and CSIC, Valencia, Spain
[168] Department of Physics, University of British Columbia, Vancouver BC, Canada
[169] Department of Physics and Astronomy, University of Victoria, Victoria BC, Canada
[170] Waseda University, Tokyo, Japan
[171] Department of Particle Physics, The Weizmann Institute of Science, Rehovot, Israel
[172] Department of Physics, University of Wisconsin, Madison WI, United States of America
[173] Fakultät für Physik und Astronomie, Julius-Maximilians-Universität, Würzburg, Germany
[174] Fachbereich C Physik, Bergische Universität Wuppertal, Wuppertal, Germany
[175] Department of Physics, Yale University, New Haven CT, United States of America
[176] Yerevan Physics Institute, Yerevan, Armenia
[177] Domaine scientifique de la Doua, Centre de Calcul CNRS/IN2P3, Villeurbanne Cedex, France
[a] Also at Laboratorio de Instrumentacao e Fisica Experimental de Particulas - LIP, Lisboa, Portugal

[b] Also at Faculdade de Ciencias and CFNUL, Universidade de Lisboa, Lisboa, Portugal
[c] Also at Particle Physics Department, Rutherford Appleton Laboratory, Didcot, United Kingdom
[d] Also at CPPM, Aix-Marseille Université and CNRS/IN2P3, Marseille, France
[e] Also at TRIUMF, Vancouver BC, Canada
[f] Also at Department of Physics, California State University, Fresno CA, United States of America
[g] Also at Faculty of Physics and Applied Computer Science, AGH-University of Science and Technology, Krakow, Poland
[h] Also at Department of Physics, University of Coimbra, Coimbra, Portugal
[i] Also at Università di Napoli Parthenope, Napoli, Italy
[j] Also at Institute of Particle Physics (IPP), Canada
[k] Also at Department of Physics, Middle East Technical University, Ankara, Turkey
[l] Also at Louisiana Tech University, Ruston LA, United States of America
[m] Also at Group of Particle Physics, University of Montreal, Montreal QC, Canada
[n] Also at Institute of Physics, Azerbaijan Academy of Sciences, Baku, Azerbaijan
[o] Also at Institut für Experimentalphysik, Universität Hamburg, Hamburg, Germany
[p] Also at Manhattan College, New York NY, United States of America
[q] Also at School of Physics and Engineering, Sun Yat-sen University, Guanzhou, China
[r] Also at Academia Sinica Grid Computing, Institute of Physics, Academia Sinica, Taipei, Taiwan
[s] Also at High Energy Physics Group, Shandong University, Shandong, China
[t] Also at California Institute of Technology, Pasadena CA, United States of America
[u] Also at Section de Physique, Université de Genève, Geneva, Switzerland
[v] Also at Departamento de Fisica, Universidade de Minho, Braga, Portugal
[w] Also at Department of Physics and Astronomy, University of South Carolina, Columbia SC, United States of America
[x] Also at KFKI Research Institute for Particle and Nuclear Physics, Budapest, Hungary
[y] Also at Institute of Physics, Jagiellonian University, Krakow, Poland
[z] Also at Department of Physics, Oxford University, Oxford, United Kingdom
[aa] Also at Institute of Physics, Academia Sinica, Taipei, Taiwan
[ab] Also at Department of Physics, The University of Michigan, Ann Arbor MI, United States of America
[ac] Also at DSM/IRFU (Institut de Recherches sur les Lois Fondamentales de l'Univers), CEA Saclay (Commissariat a l'Energie Atomique), Gif-sur-Yvette, France
[ad] Also at Laboratoire de Physique Nucléaire et de Hautes Energies, UPMC and Université Paris-Diderot and CNRS/IN2P3, Paris, France
[ae] Also at Department of Physics, Nanjing University, Jiangsu, China
* Deceased